

¹ A Landscape of Metabolic Changes Across Tumor Types

² Ed Reznik^{†*1,2}, Augustin Luna^{†3,4}, Bülent Arman Aksoy⁵, Eric Minwei Liu^{6,7}, Konnor La^{8,9},
³ Irina Ostrovnaya¹⁰, Chad J. Creighton^{11,12}, A. Ari Hakimi¹³ and Chris Sander^{*2,3}

⁴ Address: ¹Center for Molecular Oncology, Memorial Sloan Kettering Cancer Center, 1275 York
⁵ Avenue, New York, NY 10065, USA; ²Department of Epidemiology and Biostatistics, Memorial
⁶ Sloan Kettering Cancer Center, 1275 York Avenue, New York, NY 10065, USA; ³cBio Center, De-
⁷ partment of Biostatistics and Computational Biology, Dana-Farber Cancer Institute, Boston, MA
⁸ 02215, USA; ⁴Department of Cell Biology, Harvard Medical School, Boston, MA 02115, USA;
⁹ ⁵Genetics and Genomics Department, Icahn School of Medicine at Mount Sinai, New York, NY,
¹⁰ 10029, USA; ⁶Department of Physiology and Biophysics, Weill Cornell Medical College, New
¹¹ York, New York 10065, USA; ⁷Institute for Computational Biomedicine, Weill Cornell Med-
¹² ical College, New York, New York 10021, USA; ⁸Center for Molecular Oncology, Memorial
¹³ Sloan Kettering Cancer Center, 1275 York Avenue, New York, NY 10065, USA; ⁹Department of
¹⁴ Physiology and Biophysics, Weill Cornell Medical College, New York, New York 10065, USA;
¹⁵ ¹⁰Department of Epidemiology and Biostatistics, Memorial Sloan Kettering Cancer Center, 1275
¹⁶ York Avenue, New York, NY 10065, USA; ¹¹Human Genome Sequencing Center, Baylor College
¹⁷ of Medicine, Houston, TX 77030, USA; ¹²Department of Medicine, Baylor College of Medicine,
¹⁸ Houston, TX 77030, USA and ¹³Urology Service, Department of Surgery, Memorial Sloan Ketter-
¹⁹ ing Cancer Center, 1275 York Avenue, New York, NY 10065, USA

²⁰ Email: Ed Reznik[†] - reznike@mskcc.org; Chris Sander - sander.research@gmail.com

²¹ * Corresponding author

²² Abstract

23 Tumor metabolism is reorganized to support proliferation in the face of increased growth-related
24 stress. In contrast to the widespread profiling of changes to metabolic enzyme levels in cancer,
25 comparatively less attention has been paid to the substrates/products of enzyme-catalyzed reac-
26 tions, small-molecule metabolites. Here, we developed an informatic pipeline to concurrently ana-
27 lyze metabolomics data from over 900 tissue samples spanning 7 cancer types, revealing extensive
28 heterogeneity in metabolic changes across cancers of different tissues of origin. Despite this het-
29 erogeneity, a number of metabolites were recurrently differentially abundant across many cancers,
30 such as lactate and acyl-carnitine species. Through joint analysis of metabolomic data alongside
31 clinical features of patient samples, we also identified a small number of metabolites, including
32 several polyamines and kynurenine, which were recurrently associated with aggressive tumor fea-
33 tures across several tumor types. Our findings offer a glimpse onto common patterns of metabolic
34 reprogramming across cancers, and the work serves as a large-scale resource accessible via a web
35 application.

36 **Keywords**

37 cancer metabolism; metabolomics; genomics; clinical data, meta-analysis

38 **Introduction**

39 Profiling the genomes, epigenomes, and proteomes of large cohorts of tumors has generated a
40 detailed census of hallmark molecular alterations evident across many tumor types and likely to
41 drive cancer progression [1]. These findings have contributed to a holistic understanding of can-
42 cer and have elucidated novel and potentially targetable vulnerabilities. In contrast, while altered
43 metabolism is a well-accepted hallmark of cancer [2,3], the technical challenges of measuring the
44 abundance of metabolites (*e.g.* using mass spectrometry) have limited the use of metabolomic pro-
45 filing in studies of cancer tissues. Instead, much of the work in cancer metabolism has focused on
46 examination of changes in the expression of metabolic enzymes, and the identification of patterns
47 of metabolic gene expression common to many cancer types [4-6]. **In contrast, metabolomic stud-**

48 ies of cancer have been largely limited to *in vitro* flux studies of central carbon metabolism, and
49 larger metabolomic studies focused on individual cancer types [7-12], with notable and ever-more
50 frequent exceptions [13,14].

51 Tumors grow and divide in the presence of stress imposed by proliferation and augmented by cy-
52 totoxic and targeted therapy. To survive, the activity of metabolic pathways is modulated to meet
53 energetic demands, produce suitable levels of biosynthetic precursors, sustain redox potential and
54 maintain epigenetic integrity. As a whole, these metabolic alterations are implemented via changes
55 in the levels of intracellular metabolites, enzymes, and transporters [15,16]. As with genetic al-
56 terations, these metabolic alterations may differ substantially according to, among other factors,
57 the tissue-of-origin and stage of disease. Furthermore, many functional and common genetic alter-
58 ations in cancer involve metabolic enzymes (*e.g.* IDH, SDH, FH) or regulators of metabolism (*e.g.*
59 MTOR, VHL) [17-19]. In contrast, in this study, we seek to derive some organizing principles
60 for how tumors alter their metabolomes, the repertoire of intracellular, small molecule metabolites
61 constituting the cell.

62 Our work focuses on analysis of published mass-spectrometry (MS)-based metabolomic profiling
63 data of cancer tissues. Integration of MS measurements from different labs is inherently difficult
64 because of incomplete/inconsistent measurement conditions and normalization procedures between
65 different labs. To overcome this limitation, we use meta-analysis, *i.e.* metabolomic data is ana-
66 lyzed separately within each dataset, and the results of the individual analyses are subsequently
67 combined. This approach enables us to determine if different cancers exhibit common patterns of
68 metabolic changes between tumor and normal tissues. By additionally integrating clinical features
69 into our analysis (*e.g.* pathological grade of the tumor), we are able to examine the association be-
70 tween tissue metabolite levels and the clinically aggressive features of a tumor. Unlike other re-
71 cent analyses, this approach produces a single merged dataset with standardized nomenclature and
72 data. This dataset, the informatic pipeline used to produce it, and all analysis code is made publicly
73 available at https://github.com/dfc1/pancanmet_analysis for future work. An accompanying website

74 (<http://sanderlab.org/pancanmet/>) is provided to allow readers to explore the dataset, including 1)
75 univariate and bivariate change in metabolite levels and 2) clinical associations by metabolite and
76 by study. The Supplementary Data also contains tables facilitating mapping metabolites to various
77 database identifiers.

78 **Assembly of a Cross-Cancer Compendium of Metabolomics Data**

79 The first step of our analysis was to develop a computational framework to jointly analyze
80 metabolomic data produced from different laboratories. We obtained published cancer tissue
81 metabolomics data from 11 studies covering 7 distinct cancer types (see Figure 1, Figure S1, and
82 Supplementary Table 1: Merged Metabolomics). Data for all studies was collected by the original
83 investigators using mass spectrometry. Three cancer types (breast, prostate, and pancreatic ductal
84 adenocarcinoma) were represented by at least 2 different datasets, enabling us to evaluate the con-
85 sistency of findings across different studies. In total, our dataset encompasses 928 tissue samples.

86 Usage of metabolomics data for the purpose of meta-analyses involves unique technical and in-
87 formatic challenges. Unlike genomic sequencing, which frequently covers the full breadth of the
88 exome or genome, metabolomics relies on the identification of a small (on the order of hundreds)
89 library of compounds. Each individual metabolomic study is likely to profile distinct assortments
90 of these molecules [20]. Therefore, molecules profiled in one study may partially overlap the set of
91 molecules profiled in other studies, and inconsistent use of standard nomenclature for metabolites
92 makes their “alignment” across studies challenging. For example, lactate is synonymously referred
93 to as lactic acid and (S)-2-Hydroxypropanoate, and is reported alongside many other database iden-
94 tifiers (*e.g.* KEGG IDs, HMDB IDs, PubChem IDs) [21-23]. Furthermore, metabolite abundances
95 are commonly reported in relative, rather than absolute, units (*i.e.* peak intensities). Because many
96 metabolites were often at sufficiently low abundance so as to fall outside the sensitivity of the mea-
97 suring apparatus, these abundances were often imputed.

98 Technical limitations and inconsistent use of common standards render infeasible the direct com-
99 parison of raw MS-based data of metabolite levels from different laboratories. Nevertheless,
100 there is a clear missed opportunity for analyzing such data jointly, *e.g.* for discovering common
101 metabolic changes across cancer types. To overcome the technical issues associated with nor-
102 malizing raw mass spectra from different labs, we elected to use pre-normalized, published data,
103 and to apply a series of tools to make comparison between them possible. Each of the datasets
104 we used provided metabolite abundances normalized by the original investigators, but which (in
105 3/11 studies) lacked imputation or were un-standardized (here, by standardized we specifically
106 mean the data was on a scale unsuitable for visualization, *not* that the data was not un-normalized).
107 For metabolomic data which was already imputed and standardized by the original investigators,
108 we left the data unaltered. For the studies where this was not the case, we imputed any missing
109 measurements for a compound with the minimum measured value of that compound. To simplify
110 data visualization, we then divided all measurements of the compound by the median abundance
111 of that compound within the study (for further details, see Figure 2, Methods and code at https://github.com/dfci/pancanmet_analysis). All downstream analysis of the processed metabolomics
112 data (*e.g.* differential abundance tests) then relied on (1) use of non-parametric statistical methods,
113 which do not make assumptions on the underlying distribution of the data, and (2) the use of nor-
114 mal tissues as a “reference” by which to identify cancer-specific changes in metabolite abundance.
115 Importantly, while our pipeline is robust to variation in the underlying distribution of the data, erro-
116 neous normalization by the original producers of the data will (obviously) lead to erroneous results
117 from our pipeline.

119 The product of our computational pipeline is a merged metabolomics dataset containing data and
120 samples from all studies and additional metadata (Figure S1, Supplementary Table 1 Merged
121 Metabolomics) including mappings to identifiers of several key databases (*i.e.* CHEBI, KEGG,
122 HMDB, and PubChem CID) found in Supplementary Table 1: Merged IDs . Because ambiguous
123 nomenclature from each individual dataset is resolved, metabolites which are measured across
124 many studies are aligned and can be compared with meta-analysis. Access to the study data is

125 available for interactive data exploration at the project website <http://sanderlab.org/pancanmet>.
126 On this website, users may explore the data by visualizing univariate and bivariate relationships,
127 changes in abundance between tumor and normal samples across user-selected sets of metabolites,
128 associations between the available clinical data and metabolite levels, as well as exploring drug
129 compounds that target enzymatic processes used to synthesize the metabolites.

130 **Analysis of Metabolic Variation in Tumors and Normal Tissue**

131 We first sought to understand the extent to which each cohort of tumors differed from normal tis-
132 sue. In analogy to prior studies of genetic changes across cancers, we expected that some tumor
133 types may show relatively few metabolic changes compared to normal tissues, while others may
134 show many.

135 Therefore, on a study-by-study basis, we examined which metabolites were differentially abun-
136 dant between tumor/metastasis and normal samples (Mann-Whitney U test, BH-corrected p-value
137 < 0.05). For the three cancer types for which we had replicate studies, changes in abundance across
138 the studies were in good agreement (Figure S2). To further corroborate whether our differential
139 abundance findings (and the data in general) reflect true biological differences or are artifacts of
140 technical noise, we took advantage of detailed knowledge on metabolic network structure. We
141 asked whether the levels of metabolites which are adjacent in the metabolic network (*i.e.* are sub-
142 strates/products for a common enzyme) are more likely to be correlated to each other than non-
143 adjacent metabolites. We expected that, if technical noise in the data was not excessive, we would
144 see an enrichment for high positive correlations in adjacent metabolite pairs. Applying this analysis
145 to each data set in our study, we found that in all but one data set (Bladder), adjacent metabolites
146 were significantly more correlated than non-adjacent metabolites (Figure S2 SI Table 1: Covaria-
147 tion_Results).

148 The proportion of differentially abundant metabolites varied substantially from one cancer type to

the next (Figure 3A). When using the multiple-hypothesis-adjusted Mann-Whitney p-value as the only criterion for significance (*i.e.* ignoring the magnitude of change) over 60% of metabolites in both breast cancer studies and the kidney cancer study were differentially abundant. In contrast, pancreatic cancers showed characteristically fewer differentially abundant metabolites (< 20% in 2/3 studies, Supplementary Table 1: Differential Abundance Summary). Additional filtering was used to lower the proportion of differentially abundant metabolites, but the cancer-specific pattern of changes was maintained. We tested whether the large variation in propensity for differential abundance arose due to sample-size effects, and we did not find evidence to support this hypothesis (Figure S3).

This analysis revealed a cancer-type-dependent trend towards unequal proportions of metabolites which increased or decreased between tumor and normal tissues. In both breast cancer studies, we found that nearly all metabolites deemed differentially abundant were at higher levels in tumor tissue, compared to normal tissue. Similar results were reported in the original publications for these two datasets [24,25]. While biases were evident in other studies (*e.g.* differentially abundant metabolites in pancreatic tumors were more frequently depleted than accumulated in tumors), the effect was particularly striking for breast cancer. **Although it is not possible for us to determine the source of this effect, we speculate it could arise from the disproportionate extent of data imputation for metabolites in normal breast tissue, compared to the extent of imputation in tumor tissue (Figure S1).** Because the effect is replicated in both breast cancer studies, it may be possible that metabolites are broadly at higher concentrations in breast tumor compared to benign breast tissue.

It is also possible that tumor and normal tissues differ in the inherent variability of metabolite levels, without exhibiting differential abundance. To test this possibility, we compared the median absolute deviation (MAD, a non-parametric measure of the variability of a collection of measurements) of a metabolite for tumor and normal samples in each study. To control for potential biases in the relative numbers of tumor and normal samples, only data with matched tumor and adjacent-normal samples from the same patient was used. The distribution of MAD ratios over all metabo-

lites for a given cancer type indicates whether metabolite levels were inherently more variable in tumors (distribution shifted to the right of zero) or less variable in tumors (distribution shifted to the left) compared to normal tissue (Figure 3C). We again observed significant differences in variability across tumor types: breast and kidney tumors were significantly more variable than their normal tissue counterparts (Mann-Whitney $p < 0.05$). In contrast, in 2/3 pancreatic tumor datasets, tumors were significantly less variable than their normal tissue counterparts. Together with the results above, these results speak to the major differences in both absolute metabolite levels and in inherent metabolic variability associated with each individual cancer type.

Common Patterns of Metabolic Alterations Across Cancers

Cancers share common genetic alterations despite inherent physiological and molecular differences in their cell of origin. Understanding these commonalities across cancer types has expanded our understanding of the operation of molecular processes and the coordination of disparate cellular pathways [26,27]. Furthermore, it has fundamentally changed our perspective on how patients are treated and recruited to clinical trials [28]. Previously, because of a lack of data, it has not been possible to assess whether metabolic alterations, manifested through shifts in the abundances of metabolites from tumors to normal tissue, were also common across different cancer types. With the dataset organized for this work, we can begin to address this question.

Unlike the prior analysis, we now focused on analyzing common metabolomic changes across cancers of different tissues of origin. We identified 27 metabolites differentially abundant in at least 6 studies (BH-corrected p -value < 0.05 , Figure 3B and Figure 4, Supplementary Table 1: Differential Abundance Summary). Among these, a single metabolite, taurine, was differentially abundant in nine of the ten studies in which it was measured (increased in tumors in 6 studies, decreased in tumors in 3 studies, Figure 3B). Only a handful of metabolites were uniformly elevated in 5 or more studies (with no findings of significant depletion in any tumor type): four acyl-carnitine species (acetyl-, butyryl-, hexanoyl-, and octanoyl-), carnitine itself, beta-alanine, 5,6-dihydrouracil, cit-

200 rulline, kynurenone, and lactate (Supplementary Table 1: DifferentialAbundanceSummary). Com-
201 paratively fewer metabolites showed a tendency towards recurrent depletion in cancers. Four
202 metabolites, including three medium chain fatty acids (pelargonate, caprate, and laurate), were
203 depleted in 4 different studies. These results were in good agreement with a recent meta-analysis
204 (see Figure S4) [14], e.g. recurrent elevation of lactate and taurine, depletion of myo-inositol, and
205 a general elevation (rather than depletion) of metabolites in tumors compared to normal tissue. In-
206 terestingly, Goveia and colleagues [14] observed substantially more frequent elevation of various
207 amino acids (e.g. serine, arginine) than we do here, which may in part be due to their broader cov-
208 erage of cancer types.

209 Among the metabolites which showed recurrent differential abundance, several have been previ-
210 ously implicated in the development or progression of cancer. Perhaps, the best studied example is
211 lactate, the terminal product of the high-flux, energy- and precursor-producing pathway of glycoly-
212 sis, and the metabolite originally described by Otto Warburg as elevated in cancerous tissues [3]. In
213 contrast to the changes in lactate, which are likely associated with a fundamental rearrangement of
214 energy metabolism in cancer cells, the elevation of kynurenone in many cancer cells is likely not a
215 reflection of changes to energetic demands. Instead, kynurenone is a derivative of tryptophan which
216 is well-known to have immunosuppressive properties through pro-apoptotic effects when secreted
217 into the extracellular milieu, and its elevation suggests recurrent changes to the tumor microenvi-
218 ronment across many cancers [29-31].

219 Pathway-Scale Metabolic Alterations

220 An alternative approach to understanding the broad patterns of metabolic alterations is through
221 analysis of pathways into which metabolites may be organized. For each study, we mapped
222 metabolites onto KEGG pathways (Supplementary Table 1:Merged IDs), and calculated an ag-
223 gregate differential abundance score for each pathway (see Methods, Figure S5, Supplementary
224 Table 1: AllPathway). In total, 373 metabolites were identified as belonging to any given KEGG

pathway and from a collection of 246 KEGG pathways 179 (73%) were represented by at least one metabolite. Additionally, by jointly comparing KEGG and DrugBank as stored in the Pathway Commons database using the paxtoolsr R package [32], we were able to identify 70 enzymes (involved in 35 KEGG pathways) producing or consuming substrates in the current study that are targetable by 57 approved or investigational compounds present in DrugBank ([Supplementary Table 1: kegg_drugbank_results](#)) [32-34]. While a large number of pathways are represented minimally, the overall coverage of KEGG remains low with only 373 out of 3330 (11%) KEGG metabolites being represented. Because of low coverage across pathways and with many metabolites missing from each pathway (*i.e.* a high degree of missing data and low statistical power), we did not assign statistical significance to pathway-level differential abundance scores (in line with prior work [35]).

We restricted our analysis to well-represented metabolic pathways for which at least 5 metabolites in the pathway were profiled across 6 or more studies for a total of 34 pathways. Pathways associated with sugar metabolism (*e.g.* fructose/mannose metabolism, glycolysis/gluconeogenesis, and amino sugar and nucleotide sugar metabolism) were generally elevated. Many tumor types also showed increases in glutathione metabolism, which produces the critical cellular antioxidant reduced glutathione (GSH) [36]. A single pathway, fatty acid biosynthesis, showed weak, but recurrent depletion of its constituent metabolites across cancers and mirrors the increase of various acyl-carnitines across many cancer types (Figure 3). Acyl-carnitines are generated by beta-oxidation of fatty acids and are used to refuel the TCA cycle with acetyl-CoA. Our data suggests that the general elevation of acyl-carnitines and the concurrent depletion of medium chain fatty acids in tumors may reflect an increased reliance on fatty acid catabolism to replenish the TCA cycle in cancer.

A central problem in metabolism research is understanding the connection between metabolite levels and the fluxes of reactions involving those metabolites as substrates/products. In general, flux through a metabolic reaction is dependent (in a complex, nonlinear fashion) on (1) the levels of substrates/products of the reaction, (2) the levels of the enzyme catalyzing the reaction, and (3) the network context, (*i.e.* the kinetics of the reactions surrounding the flux of interest in the metabolic

network). For example, it is not necessarily true that an increase in the levels of a substrate will increase flux through the corresponding enzyme (*e.g.* if fluxes downstream are reduced, this may induce a bottleneck and accumulation of the metabolite). Due to this complexity, the inference of fluxes from metabolite levels remains unresolved and has been the focus of numerous studies from our group and others [37-39]. Despite these challenges, drawing inferences on changes in flux from the pattern of metabolite changes is instructive for understanding high-level changes in metabolism, and critical for generating experimentally testable hypotheses regarding metabolic flux.

With the above caveats in mind, we began to dissect the patterns of metabolite changes in glycolysis and the TCA cycle, which in addition to producing NADH/FADH₂/ATP generate high volumes of metabolic building blocks for biosynthesis (Figure 5). We first noted that while lactate levels are commonly elevated across most cancers, the remaining metabolites in glycolysis were in general not also elevated. To evaluate if the changes in metabolite abundances were synchronized across samples, we calculated the correlation between metabolites in glycolysis and lactate. We observed that levels of metabolites in upper glycolysis (*e.g.* G6P and F6P) and 3-phosphoglycerate were frequently correlated to levels of lactate across most cancer types. In contrast, 2-phosphoglycerate and phosphoenolpyruvate were commonly not positively correlated or negatively correlated to levels of lactate. Taken together, the (1) prevalence of coordinated changes in metabolites from upper glycolysis with lactate, (2) increase in lactate levels in 6/9 studies, and (3) increases in levels of phosphorylated glucose (G6P) in 4/8 studies, suggests that increases in lactate levels may be attributed to increases in glucose uptake and phosphorylation, and increases in glycolytic flux and excretion of lactate. As others have pointed out [3], such an increase in glycolytic flux may provide additional carbon (via overflow into peripheral biosynthetic pathways) needed for growth. Interestingly, one cancer type (clear cell kidney) showed a strong (Spearman rho -.6, p-value < 10⁻¹⁴) anti-correlation between levels of citrate and lactate. Clear cell kidney tumors are known to be highly HIF-activated, which can induce phosphorylation and inactivation of PDH via the action of PDK and lead to preferential shunting of pyruvate into lactate rather than into the TCA cycle.

278 Unexpected patterns related to tissue-of-origin also emerged when contrasting the pattern of
279 metabolomic changes in central carbon metabolism across cancer types. For example, both prostate
280 cancer studies support a drop in citrate levels in prostate tumors compared to normal tissue, a fea-
281 ture which is not evident in any other cancer type. This is in agreement with prior research show-
282 ing that while normal prostate glandular epithelium secretes large amounts of citrate, depletion
283 of zinc (an inhibitor of mitochondrial aconitase) relieves a “metabolic bottleneck” and leads to
284 an increase in the oxidation of citrate/conitase to isocitrate [40]. Similarly, clear cell kidney tu-
285 mors are the only cancer type to show an increase in metabolites upstream of SDH in the TCA cy-
286 cle (succinate, citrate, aconitate) and depletion of metabolites downstream of SDH (fumarate and
287 malate). These tumors are known to be highly depleted of mitochondrial DNA and RNA [41,42],
288 which suppresses the activity of the mitochondrial respiratory chain and consequently Complex
289 II/SDH. We propose that the sudden shift in metabolite patterns at SDH in clear cell kidney tumors
290 may therefore arise from a bottleneck associated with suppression of the mitochondrial respiratory
291 chain.

292 In some ways, the depiction of metabolomic changes in Figure 5A is misleading; while an increase
293 in the abundance of a metabolite may be evident in aggregate across all samples, there may re-
294 main individual tumors which are depleted of that metabolite. To better understand the nature of
295 elevated lactate levels in tumors, we leveraged a unique part of our data: 343 matched pairs of
296 tumor/adjacent-normal tissue samples (*i.e.* each such pair was derived from the same patient).
297 While both a paired and unpaired analysis are informative, a paired analysis normalizes for po-
298 tential patient-to-patient variation (independent of tumor-to-normal variation) in the levels of a
299 metabolite. Despite elevation of lactate in 6/9 studies, 82/343 (24%) paired tumor/normal samples
300 contained lower levels of lactate than their matched normal tissue counterpart. While most cancer
301 types were enriched for tumors with increased levels of lactate, prostate tumors were the outliers:
302 the majority of prostate tumors showed reduced levels of lactate relative to paired adjacent nor-
303 mal tissue. Nevertheless, all studies showed > 10% of samples with depleted lactate levels relative
304 to normal tissue (*e.g.* 32/138 ≈ 23% of kidney cancer pairs). This heterogeneity in lactate levels

305 compared to normal tissue may partially explain the cancer-type-specific utility and indication for
306 FDG-PET imaging, which relies on elevated glucose uptake (and potentially an increased rate of
307 lactate production) to visualize tumors [43]. Interestingly, when repeating the paired analysis above
308 on all metabolites, we found that lactate was the third most frequently elevated metabolite, behind
309 glutamate and kynureanine (Figure 5C).

310 Metabolic Indicators of Tumor Progression

311 Tumors become clinically aggressive by acquiring genetic, physiological, and morphological fea-
312 tures that enable them to invade foreign tissues and metastasize. Therefore, we examined our data
313 for metabolic signals associated with progression of tumors to higher grade, a histological measure
314 of the extent of abnormal appearance of tumor cells. **Although clinical data was sparsely reported**
315 **in the studies we examined, 5 studies reported data on clinical stage or grade, with a greater num-**
316 **ber of data points available for tumor grade (Supplementary Table 1: ClinFeatures). Importantly,**
317 **while tumor grading systems vary from one cancer type to the next, the principle underlying grad-**
318 **ing (examining the abnormal appearance of a cell) is common across all cancer types: higher grade**
319 **tumors are more aggressive.** Because of the decreased statistical power associated with looking for
320 associations between metabolite levels and subsets of our tumor data, we adopted a meta-analysis
321 approach. We identified metabolites which showed recurrent increases/decreases in metabolite
322 levels with increasing tumor grade across several cancer types. **As before, our meta-analysis ap-**
323 **proach relies strictly on non-parametric methods (that do not make assumptions about the under-**
324 **lying distribution of the data) and is suitable for the metabolomics data used here.** Furthermore,
325 we designed our analysis to account for the frequency of imputed data for each metabolite under
326 consideration (see detailed description in Methods).

327 In total, we found 174 tumor tissue metabolites whose abundance were significantly correlated
328 to tumor grade (BH-adjusted meta-p-value < 0.05, Supplementary Table 2). Filtering these *post-*
329 *hoc* results further to extract metabolites significantly associated with clinical features across

330 many tumor types, we found 4 metabolites (spermidine, uracil, 3-aminoisobutyrate, and 2-
331 hydroxyglutarate) associated with tumor grade in at least 4 studies, and 57 metabolites associated
332 with tumor grade in 3 studies. Notably, the number of metabolites significantly associated with
333 grade in each study (*post-hoc*) was correlated to the number of samples in the study with clinical
334 data, suggesting that this analysis may be biased toward studies with larger samples sizes (Figure
335 S3). Notably, spermidine showed a significant association with tumor grade across four different
336 cancer types (breast, kidney, brain, and prostate cancer) (Figure 6A). Spermidine is a polyamine; a
337 class of molecules essential for eukaryotic cell growth as well as tumorigenesis [44]. Furthermore,
338 spermidine has been reported as a potential biomarker for prostate cancer aggressiveness [45]. In
339 many cases the direction of association for a single metabolite often varied between cancer types.
340 For example, 2-hydroxyglutarate was associated with increased grade in breast and kidney tumors,
341 but decreased grade in glioma and prostate tumors. We speculate that differences both in genetic
342 background, as well as in chemical identity, may explain the discordant associations between 2-HG
343 and tumor grade. Specifically, in gliomas, the D- enantiomer of 2-HG is produced by neomorphic
344 *IDH* mutations, which are themselves associated with a better prognosis. In contrast, the more po-
345 tent (in terms of inhibitory capacity) L- enantiomer of 2-HG, whose production is induced by hy-
346 poxia [46], is likely the enantiomer produced by HIF-driven clear-cell renal cell carcinomas [47].
347 To evaluate whether differences in the stereoisomeric identity of 2-HG actually account for the
348 differences in association with grade, further enantiomer-specific metabolite profiling will be re-
349 quired.

350 Among our findings was the observation that kynurenine levels in tumor samples were asso-
351 ciated with increased tumor grade in three studies (Figure 6B), Breast Terunuma, Glioma, and
352 Prostate Sreekumar, uncorrected p-value < 0.05, meta p-value < 10^{-4}), and was trending toward
353 significance in the other prostate study (uncorrected p-value 0.097). Kynurenine is a metabolic
354 byproduct of the degradation of tryptophan by two groups of enzymes: tryptophan dioxygenases
355 and indoleamine 2,3-dioxogenases [29]. Binding of kynurenine to aryl hydrocarbon receptors
356 (AHRs) suppresses the activity of T-effector cells, as well as indirectly activating regulatory pro-

357 tumorigenic T cells [48]. Kynurenine was particularly unique in our meta-analysis because it was
358 found to be elevated (compared to normal tissue) in 8/10 studies, and in 7/8 of these. In these stud-
359 ies, it was more than double the abundance of that found in normal tissue; thus, kynurenine seems
360 to be not only a recurrent differentiating feature of tumor tissue, but also a potential marker of dis-
361 ease progression in cancer and other diseases [49-51].

362 The normal tissue and microenvironment surrounding the tumor plays a key role in the develop-
363 ment of cancers [52-54]. It is therefore possible that the metabolic demands of a tumor can drive a
364 physiological change in the metabolism of nearby normal tissue. Therefore, we repeated our meta-
365 analysis above, focusing on the association between metabolite levels in the adjacent normal tissue
366 and the pathological grade of the matched tumor. We identified 4 metabolites which were asso-
367 ciated with tumor grade: putrescine, galactose, and 2 fatty acids (margarate and stearate) (uncor-
368 rected individual study p-value < 0.05 in at least 2 studies, BH-corrected meta-p-value < .1). For
369 putrescine, another polyamine, increased levels in normal tissue were associated with higher grade
370 in both kidney and prostate cancers. Of clinical relevance, 2-difluoromethylornithine (DFMO) is
371 an enzymatic inhibitor of ornithine decarboxylase of necessary for the production of both spermi-
372 dine and putrescine [55], and there is some evidence that it may be useful in treatment of a variety
373 of cancers (colorectal, melanoma) as well as a part of combinatorial treatments of brain cancers
374 [56]. Interestingly, clinical associations in normal tissue were sometimes, but not always, mirrored
375 in the analogous tumor tissue (Figure S6A). While many metabolites (*e.g.* choline) showed com-
376 mon patterns of association in kidney tumor and normal tissue (and less frequently in breast and
377 prostate tissues), other metabolites showed opposing associations (*e.g.* spermidine in prostate tu-
378 mors/normal tissues, Figure 6).

379 What is a plausible interpretation of the connection between normal tissue metabolism and ag-
380 gressive tumor features? One explanation is that the nearby tissue changes physiologically in the
381 course of tumor progression, for example in response to cytotoxic therapies. Another, more in-
382 triguering, possibility is that there may some interaction between tumor cells and the surrounding

383 normal tissue. To evaluate if this may be the case, we again used metabolite data on 343 matched
384 tumor/normal pairs from the same patient, and evaluated (study-by-study) whether metabolite lev-
385 els in tumor and normal tissue were correlated. Of the 205 metabolites measured in at least 5/8
386 studies with paired samples, we identified 8 metabolites which were recurrently correlated between
387 tumor/normal tissues in at least 5 studies (Supplementary Table 1: Pairscores). Of these, a num-
388 ber were metabolites which circulate physiologically through the body (*e.g.* 1,5-anhydroglucitol,
389 3-hydroxybutyrate, urea). Thus, our data is suggestive of many correlations between tumor and
390 normal metabolite levels arising because of broad changes to the physiology of the patient. Inter-
391 estingly, however, alanine was significantly correlated between tumor and normal tissues in the
392 Pancreatic Kamphoerst study, and approached statistical significance in a second pancreatic study
393 (Pancreatic Zhang 1), possibly supporting the recent report of shuttling of alanine from nearby pan-
394 creatic stellate cells to tumor cells [57].

395 Discussion

396 Tumors are molecularly shaped by the cells from which they arise. Analogous to genetic alter-
397 ations, it is possible that the development of cancer may place common demands on cellular
398 metabolism, irrespective of the tissue of origin. Here, we offer a glimpse onto the common patterns
399 and distinguishing features of metabolic reprogramming across cancers.

400 Our approach to analyzing a compendium of small molecule data derived from mass spectrometry
401 has inherent assumptions, which we addressed to the extent possible. We relied on the normaliza-
402 tion and standardization procedures undertaken by the original researchers of a study. While all the
403 data in our study was pre-normalized, two studies contained data that was not imputed or standar-
404 dized; in those cases, we applied a simple imputation/standardization pipeline. We also implemented
405 a bioinformatic pipeline to align metabolites identified using disparate nomenclature, the code
406 repository for which is publicly available on GitHub (https://github.com/dfci/pancanmet_analysis).
407 This repository, additionally, provides code for the whole analysis described here. Finally, to com-

408 pare data across studies obeying unknown and potentially various statistical/distributional prop-
409 erties, we relied heavily on non-parametric statistics, and either (1) used changes relative to nor-
410 mal tissue as the unit of comparison or (2) non-parametrically associated changes in metabolite
411 levels with clinical data. We expect that this pipeline, through collaboration with others in the
412 metabolomics community, can be expanded and improved.

413 Our findings illustrate that cancers of widely different types share some common patterns of
414 changes to metabolite levels. A subset of metabolites, including acyl-carnitines, lactate, kynure-
415 nine, and taurine, were recurrently higher in abundance across many tumor types (when compared
416 to normal tissue). Comparatively fewer metabolites, including some fatty acids, were recurrently
417 depleted across these same cancer types. These findings echo those from a recent meta-analysis
418 of published cancer metabolomics data [14]. Importantly, the collection of metabolites displaying
419 clear, consistent shifts in abundance across cancers are in the minority. The majority of metabo-
420 lites, both in central carbon metabolism and in secondary metabolic pathways, showed heteroge-
421 neous changes across tumor types and requires exploration in future studies.

422 We also found that the metabolism of tumors is linked to their clinical presentation, and in par-
423 ticular to their grade. While it should come as no surprise that tumor metabolism necessarily ac-
424 ccommodates and supports the development of aggressive disease and metastasis, it was intriguing
425 to find that some metabolites were indicative of aggressive disease across several cancer types.
426 Our analysis also showed that the metabolism of adjacent-normal tissue, which is physiologi-
427 cally linked to the tumor by physical location and shared vasculature, is remodeled in patients
428 with high-grade tumors. **One potential explanation for the association between metabolite levels**
429 **in tumor/normal tissue and tumor grade is variation in the degree of infiltrating immune or stro-**
430 **mal cells. Such infiltration could also, for example, enrich or dilute the abundance of metabolites**
431 **specific to either tumor or immune/stromal cells. Because one study (Breast Tang) used TCGA-**
432 **profiled tissue samples, we were able to recover estimates of stromal and immune infiltration for**
433 **23 samples from this study and investigate if infiltration was correlated with metabolite levels**

434 in this study. Interestingly, while no metabolites reached statistical significance upon multiple-
435 hypothesis correction, several metabolites of high interest (*e.g.* NADH) were trending towards
436 significance (Figure S6). Given the relatively small sample size of this dataset (23 samples), we
437 speculate that improved statistical power may indeed yield metabolites indicative of or enriched in
438 various components of the tumor microenvironment.

439 In some tumor types, and in particular in clear-cell renal cell carcinomas, many metabolites showed
440 changes in abundance in normal tissue which were associated with the grade of the patient's tumor.
441 Much remains to be understood of this phenomenon, including in particular the possibility that
442 tumor and normal tissue may be shuttling nutrients between each other in order to sustain prolifer-
443 ation (*e.g.* in pancreatic stellate cells in pancreatic ductal adenocarcinoma) [57]. Importantly, ob-
444 serving (or failing to observe) a correlation between steady-state metabolite levels in tumor/normal
445 tissues is not sufficient evidence to conclude nutrient shuttling between the two tissues. Instead, the
446 precise mechanism of shuttling could lead to different kinds of correlations between tumor/normal
447 metabolites; for example, a positive correlation may arise if excess production of a metabolite in
448 the normal tissue is shuttled to the tumor passively by blood vessels. Similarly, a negative corre-
449 lation could arise if a fixed amount of metabolite produced in the normal tissue is actively trans-
450 ported to the tumor, *e.g.* by overexpression of a nutrient exporter in the normal tissue. Thus, tu-
451 mor/normal metabolite correlations should be interpreted with care.

452 One outcome of our work is a merged, standardized metabolomics dataset which can be used by
453 others in the future with an accompanying website (<http://sanderlab.org/pancanmet/>) allowing read-
454 ers to explore 1) metabolite data stratified by metadata data (*e.g.* HMDB classifications) and by
455 study, 2) univariate and bivariate changes by metabolite and by study, and 3) clinical associations
456 by metabolite and by study. The analysis in this paper has focused on non-parametric, univariate
457 analysis of changes in metabolite levels between tumor and normal samples. Yet, other analyses
458 which respect the limitations of the data (Figure 2) are possible. One example is a correlation anal-
459 ysis, akin to those proposed in several publications using gene expression data [58]. It is possible

460 that, by examination of changes in covariation patterns between metabolites between different sub-
461 sets of samples (*e.g.* tumor/normal, high grade/low grade tumors), the identification of putatively
462 “rewired” metabolic pathways may be possible. Coupling covariation analyses with other data (*e.g.*
463 transcriptomics, proteomics) may yield further insights.

464 Finally, given the proliferation of clinical genomic sequencing of cancer samples, it seems natu-
465 ral to propose that connections be drawn between genetic alterations and the metabolic landscape
466 of tumors. Several prominent examples now exist of molecular alterations which manifest with,
467 among other things, distinct metabolic phenotypes: *KRAS* mutations in pancreatic adenocarcino-
468 mas, which induce macropinocytotic scavenging of extracellular nutrients [59] and hotspot *IDH1*
469 and *IDH2* mutations which produce 2-hydroxyglutarate and induce DNA hypermethylation via
470 inhibition of α -ketoglutarate-dependent DNA demethylases [11,60]. Furthermore, recent work
471 has demonstrated that metabolic changes arising from a single common genetic lesion are tissue-
472 specific, and can vary substantially from one cancer type to the next [13]. Thus, it is likely that
473 other mutation-associated metabolic effects, perhaps subtle but nevertheless impacting tumor vi-
474 ability, remain to be uncovered.

475 Methods

476 Data Imputation and Standardization

477 All data used in this study was pre-normalized, *i.e.* no raw mass spectra were analyzed. For data
478 which was already imputed and standardized, we used the data as reported by the original authors.
479 This includes both breast studies [24,25], glioma [61], kidney [35], ovary, [62], 2 of the pancre-
480 atic studies [63], and one of the prostate studies [64]. For the bladder study [65], data was obtained
481 normalized after log transformation, with no further imputation required. For this study, normal-
482 ized data was simply re-exponentiated. For two studies, PAAD [59] and PRAD [66]) for which no
483 imputation was completed, we applied the following imputation and standardization procedure.

484 For each metabolite, imputed values were set equal to the minimum measured abundance of that
485 metabolite; additional statistics on imputed metabolites are shown in Figure S1. Then, all measure-
486 ments of the metabolite were divided by the median abundance of that metabolite. The entire data
487 import pipeline can be replicated using the code provided in the GitHub repository.

488 Metabolite ID Mapping

489 In addition to data standardization, a bioinformatic challenge in the current work was the identi-
490 fication of metabolites profiled across multiple studies. Unlike other high-throughput technolo-
491 gies which can measure the abundance of all relevant species in a sample (*e.g.* RNA sequenc-
492 ing), metabolomic profiling samples only a fraction of all compounds in the metabolite. More
493 importantly, metabolites are referred to by different synonymous names and database identifiers.

494 To address this issue, we used the Chemical Translation Service [67] to retrieve synonymous
495 identifiers of each metabolite. These identifiers were then used to assemble a meta-dataset of all
496 metabolomics data, “aligning” metabolites sharing common identifiers. Manual inspection of the
497 aligned dataset confirmed that our method correctly matched metabolites across different studies.
498 All code for data standardization and alignment is provided on GitHub (https://github.com/dfci/pancanmet_analysis).

500 These mapped identifiers were used in conjunction with the paxtoolsr R Bioconductor package to
501 map identifiers onto the Pathway Commons Version 8 database, which includes both KEGG and
502 DrugBank interactions to identify drug targetable pathways.

503 Differential Abundance Tests

504 Differential abundance was calculated using the ratio of the average abundance of a metabolite in
505 tumor tissue, to the average abundance of a metabolite in normal tissue. Statistical significance

506 was assessed using non-parametric Mann-Whitney U-tests. P-values were adjusted for multiple-
507 hypothesis testing using the Benjamini-Hochberg procedure.

508 **Pathway Differential Abundance Score**

509 The differential abundance score for a pathway was defined as

510
$$DA = \frac{I - D}{S}$$

511

512 where I is the number of measured metabolites in a pathway which increased in abundance relative
513 to normal tissue, D is the number which decreased, and S is the total number of measured metabo-
514 lites. A DA score of 1 indicates that all metabolites increased in abundance, whereas a score of -1
515 indicates that all metabolites decreased in abundance, relative to normal tissue.

516 **Calculation of Metabolic Variation (MAD Score)**

517 Metabolic variation analysis was completed for each study with paired tumor/adjacent-normal sam-
518 ples from the same patient. For each study, we restricted analysis to such paired data, and parti-
519 tioned the metabolomics data into measurements from tumor and normal tissue samples. Then, for
520 each metabolite m with measurements from n samples $X = X_1, X_2, \dots, X_n$, a normalized median ab-
521 solute deviation (MAD) was calculated according to the formula

522
$$MAD_X = \text{median}(|\log_2(X_i/\text{median}(X))|) \quad (1)$$

523

524 The MAD was calculated for each metabolite m , separately for tumor (MAD_m^T) and normal
525 (MAD_m^N) samples. The ratio of these two MAD scores for each metabolite m , $MAD_m^r = \frac{MAD_m^T}{MAD_m^N}$, was
526 then calculated. The distribution of MAD^r scores indicates whether tumor samples show signifi-
527 cantly different levels of variation than normal tissues (*i.e.* if the distribution of MAD^r scores are
528 skewed to be significantly less than 1, this indicates that tumor samples exhibit less variation than
529 normal samples). The results of the MAD analysis were invariant to the exclusion highly-imputed
530 metabolites.

531 Clinical Features

532 In general, clinical data was imported from the datasets reported by original investigators. For
533 prostate tumors specifically (Prostate Priolo and Prostate Sreekumar studies), we converted Glea-
534 son score to tumor grade as follows (3+3 = Grade 1; 3+4,4+3 = Grade 2; 4+4,5+4 = Grade 3).

535 Association with Tumor Grade

536 Different statistical tests were applied to identify correlation between metabolites and clinical fea-
537 tures depending on the level of censoring (*i.e.* imputation) in the data. If there was less than 20%
538 censoring within the tested set, the Jonckheere-Terpstra test (a non-parametric test which uses per-
539 mutations to calculate the p-value) was used to examine ordered differences among classes. If there
540 was more than 20% but less than 80% censored data, an exact log-rank trend test was used for in-
541 terval (left) censored data. Both tests assume a metabolite should increase/decrease monotonically
542 with stage/grade. If there is more than 80% censoring, no test was used, and the metabolite was
543 ignored. To summarize the tests across cohorts Fisher's method was used to combine p-values.
544 Note that resulting combined p-value is parametric. Since we were interested in finding associa-
545 tions of a common sign (*e.g.* consistently positive correlation across multiple studies), one-sided

⁵⁴⁶ p-values were calculated first, aggregated into a combined p-value using Fisher's method [68], and
⁵⁴⁷ then transformed to two-sided combined p-value.

548 Supplementary Table 1 - Merged Metabolomics Data (merged_metabolomics.csv)
549 Supplementary Table 1 - Tumor/Normal Pairs (tumor_normal_pairs.csv)
550 Supplementary Table 1 - Clinical Data (clifeatures.csv)
551 Supplementary Table 1 - Differential Abundance Results (DifferentialAbundanceSummary.csv)
552 Supplementary Table 1 - Metabolite Classifications (hmdbClassification.csv)
553 **Supplementary Table 1 - Figure S5 Data: Differential Abundance Scores (AllPath-**
554 **way_diffAbundanceBig.csv)**
555 Supplementary Table 1 - KEGG/DrugBank Pharmacology Coverage Data (kegg_drugbank_results.txt)
556
557 Supplementary Table 1 - Metabolite ID Dictionary (Sept152015/merged_IDs.csv)
558 Supplementary Table 1 - Tumor/Normal Correlation Scores (pairscores.csv)
559 Supplementary Table 1 - Adjacent Metabolite Analysis (Covariation_Results.csv)
560 Supplementary Table 2 - Clinical Data Analysis (updated results stage and grade Jan 2017
561 **max1.xlsx**)

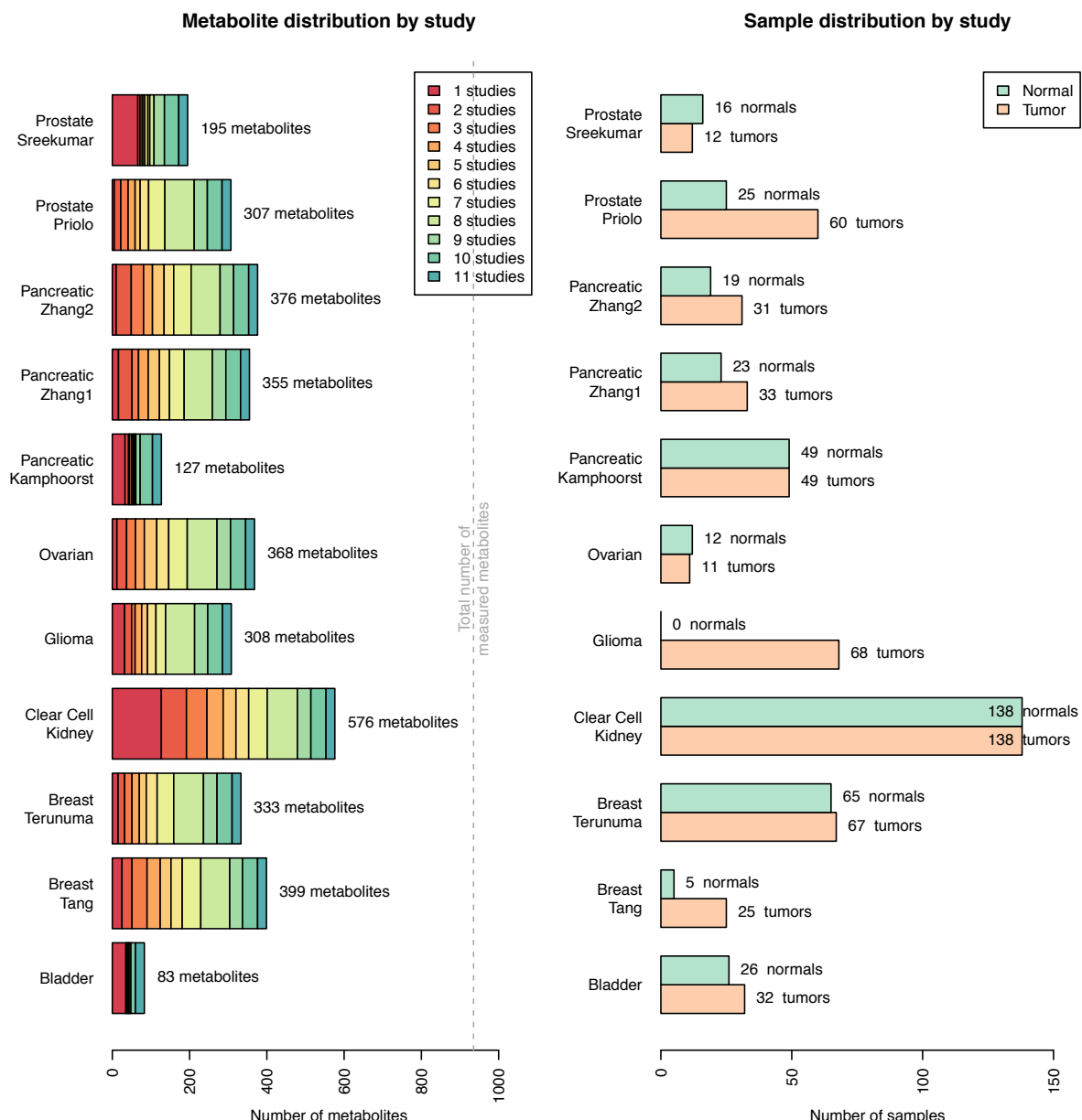


Figure 1: Metabolomics data (928 samples, 7 cancer types) analyzed in this study. Data from eleven distinct metabolomics studies were aggregated. Due to incomplete coverage of the metabolome, many metabolites were profiled in a small proportion of studies. The number of tumor/normal samples varied from study to study, and all but one study, conducted on gliomas, contained normal samples. In some, but not all cases, tumor/adjacent-normal tissue samples were collected from the same patient (*i.e.* “matched” or “paired” samples, terms used interchangeably). This matched data is indicated in the Supplementary Table 2.

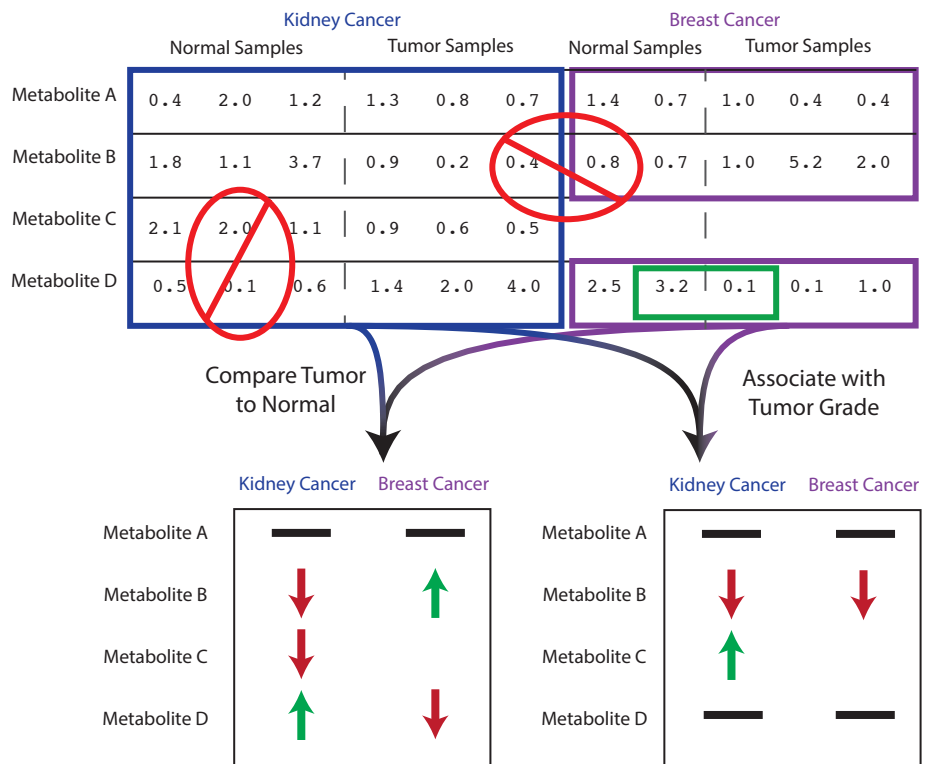


Figure 2: Workflow for the aggregation and comparison of metabolite profiles across studies. Metabolomics data collected in different laboratories is difficult to directly compare. Our approach is to analyze data from each metabolomics dataset separately (*e.g.* comparing tumor to normal samples), and then aggregate these results across cancer types. Typically, for each metabolite, abundance is reported relative to the median of all measurements of a metabolite within a study. Comparisons between different metabolites profiled in the same study is not directly possible (leftmost red oval). Furthermore, comparisons between the same metabolite profiled across different studies is not possible (topmost red oval). Throughout our analysis, we frequently examine the change in abundance of a single metabolite across different subsets of tissue samples (*e.g.* tumor/normal samples) from the same study (green oval). Correlative analysis with variables of interest (*e.g.* clinical data) is also feasible.

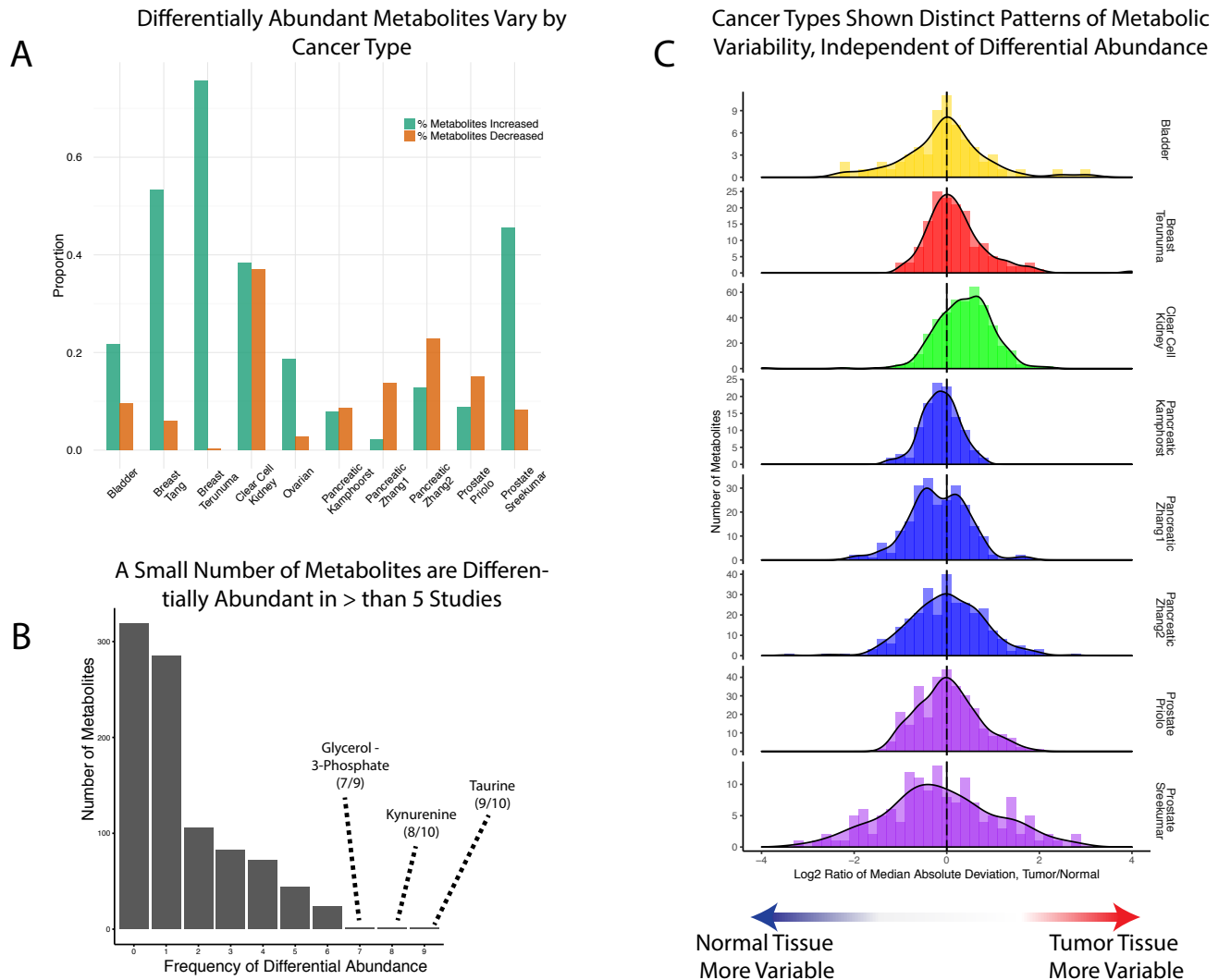


Figure 3: Differential metabolite abundances in tumor versus normal across cancer types. In total, 10/11 studies contained adjacent-normal tissue for comparison, and were included in this analysis (in total, 482 tumor samples and 378 normal samples). Analysis was done without regard to whether tumor/normal samples were paired. **(A)** Proportion of metabolites in each study which were differentially abundant in tumor vs. normal samples (BH-corrected p-value < 0.05). **(B)** The frequency of differential abundance across all metabolites. Most metabolites are rarely differentially abundant, in part because they may only be measured in a small number of studies. A small number of metabolites are often differentially abundant. **(C) Variability of metabolite levels for each study.** MAD ratio distributions show the inherent variability of metabolite levels; distributions shifted to the right of zero show a greater degree of variability in tumors compared to normal tissue, while those distributions shifted to the left show less. A total of 343 pairs of tumor/normal samples from 8 studies (Bladder, Breast Terunuma, Breast Tang, Kidney, Pancreatic Kamphoerst, Pancreatic Zhang 1, Pancreatic Zhang2, Prostate Priolo, and Prostate Sreekumar) were used.

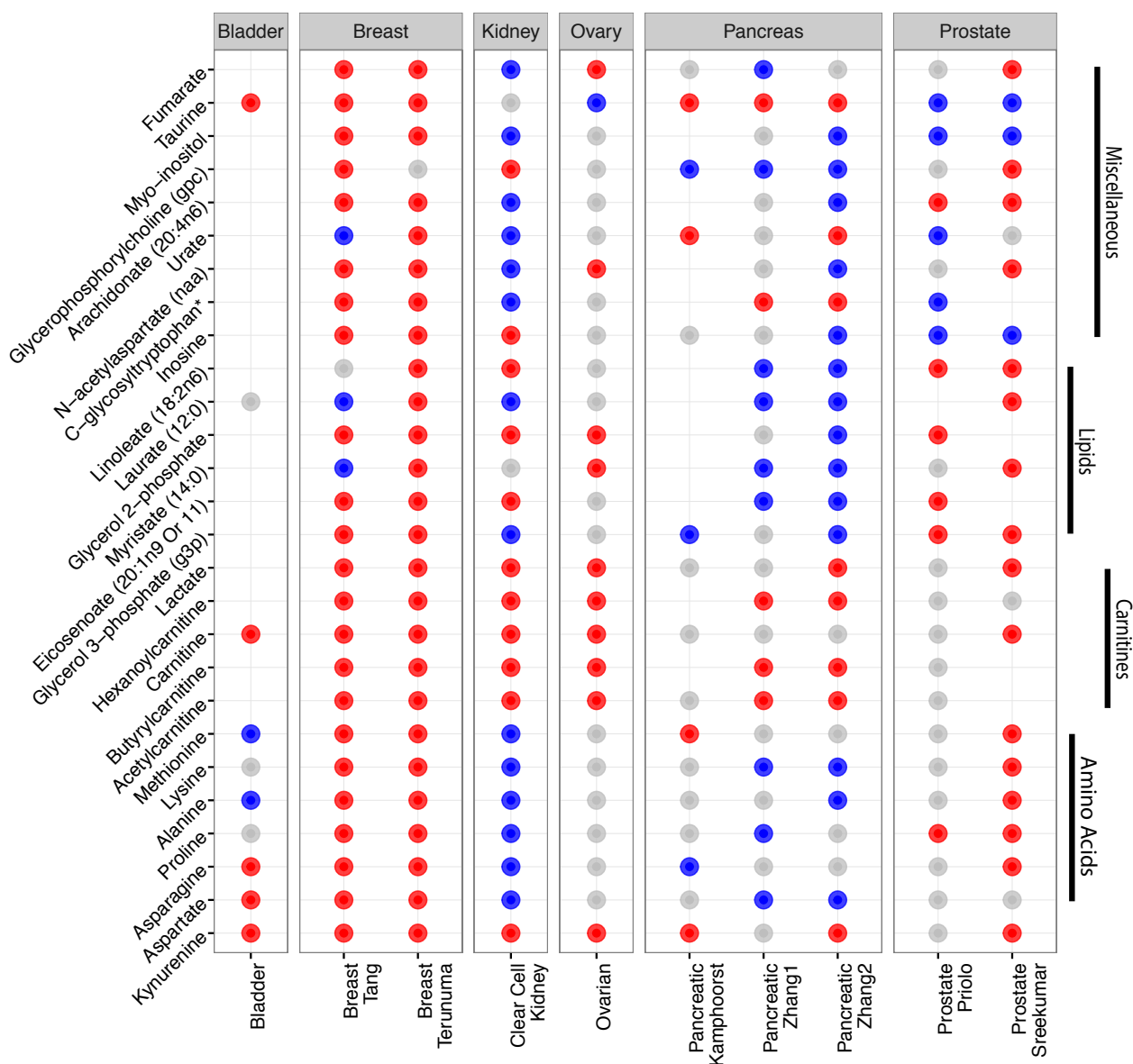


Figure 4: Differential abundance across all cancer types. Blue circles indicate metabolites depleted in tumors relative to normal tissue, red circles indicate metabolites increased in tumors relative to normal tissue). Metabolites differentially abundant in 6 or more studies are displayed.

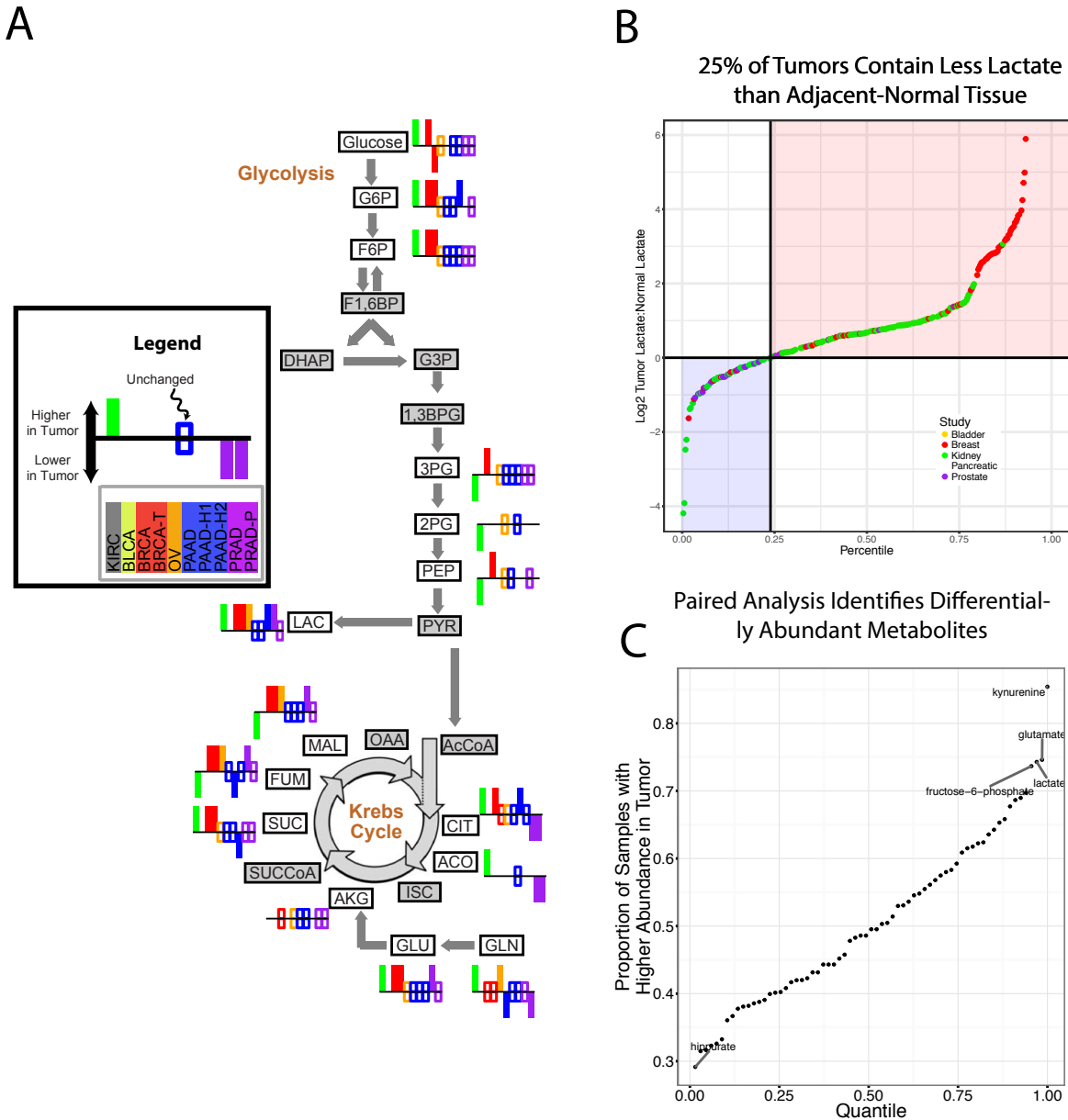
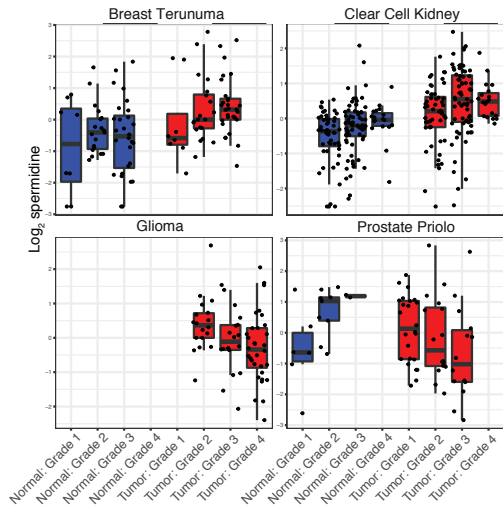


Figure 5: Central carbon metabolism across cancer types. (A) Differential abundance (tumor vs. normal) in glycolysis and the TCA cycle across many cancer types. Bars indicate whether the metabolite was higher/lower/unchanged in tumor samples compared to normal tissue; the absence of a bar means the data was missing. BRCA-T: breast data from [25], PAAD-H1/2: pancreatic data from [63], PRAD-P: prostate data from [64]. Data from 10/11 studies (LGG excluded for no normal samples, in total, 482 tumor samples and 378 normal samples). (B) Sorted \log_2 ratio of lactate levels in matched tumor/normal samples from 5 cancer types. Approximately 25% of samples have less lactate in tumors, compared to normal tissue. In both (A) and (B), analysis was done without regard to whether tumor/normal samples were paired. (C) Frequency of elevation for each metabolite across all matched tumor-normal pairs (343 pairs in total). Kynurenine is elevated in 85% of matched samples.

A Levels of Spermidine in Tumor and Normal Tissue are Associated with Tumor Grade



B Levels of Kynurenone in Tumors are Correlated with Advanced Grade

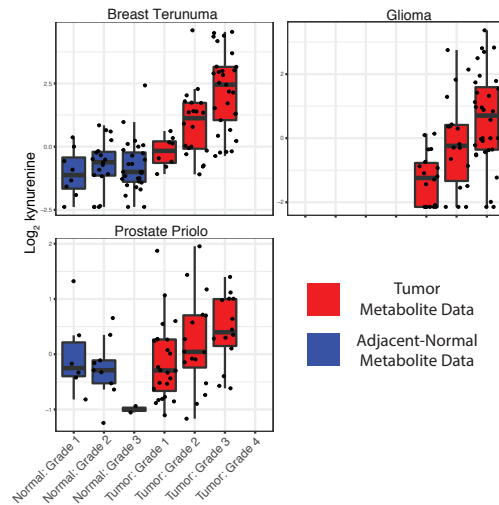


Figure 6: Metabolic correlation with tumor progression. A total of 638 of the tissue samples had some type of associated clinical data (392 tumors and 246 normal tissues from 7 studies, including Breast Terunuma, Breast Tang, Kidney, Glioma, Ovarian, Prostate Priolo, and Prostate Sreekumar). Analysis was done without regard to whether tumor/normal samples were paired. Meta-analysis identified 174 metabolites whose abundance in tumors was significantly associated to tumor grade in 1 or more metabolomics studies. **(A)** Spermidine, a polyamine involved in cell proliferation, showed a significant association with tumor grade across four different cancer types (breast, kidney, brain, and prostate cancer). **(B)** Association of kynurenone levels with tumor grade across several cancers; kynurenone is part of the tryptophan degradation pathway with pro-apoptotic effects on immune cells.

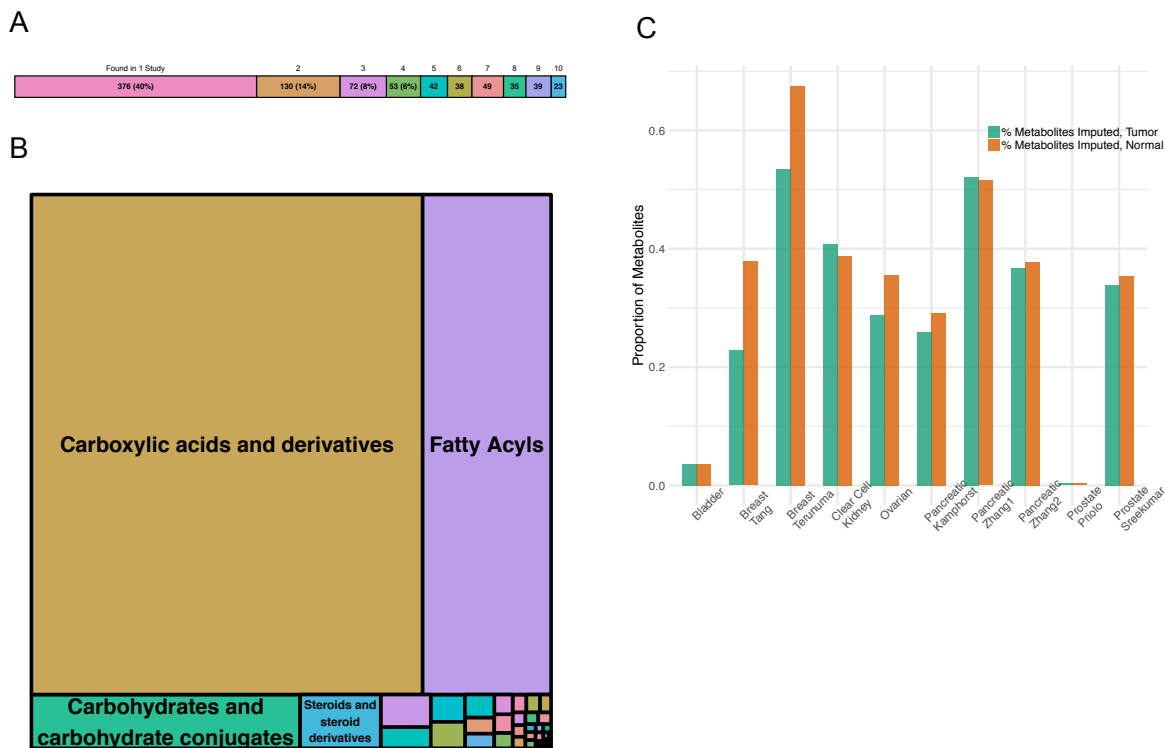


Figure S1: Summary of metabolites. (A) Number of metabolites found in multiple studies; percentile labels are not shown for study counts with less than 5% of metabolites. (B) Classification of study metabolites by Human Metabolome Database (HMDB) chemical taxonomy "Class" entries. The three largest groups of metabolites as classified using the Human Metabolome Database (HMDB) chemical taxonomy are as follows: 1) 120 carboxylic acids and derivatives of which 109 were sub-classified as amino acids, peptides, and analogues, 2) 83 fatty acyls of which 60 are sub-classified as fatty acids and conjugates, and 3) 64 carbohydrates and carbohydrate conjugates of which 22 were sub-classified as monosaccharides; classification was only conducted for metabolites that could be confidently identified using HMDB. (C) Proportion of imputed metabolites. For each study, we calculated the proportion of metabolites with greater than 20% imputation in tumor samples. The calculation was repeated separately for normal samples. The two breast studies are exceptional because of the incongruent level of imputation between normal and tumor samples: far more metabolites are heavily imputed in normal breast samples, compared breast tumor samples. In total, 10/11 studies contained adjacent-normal tissue for comparison, and were included in this analysis (in total, 482 tumor samples and 378 normal samples). Analysis was done without regard to whether tumor/normal samples were paired.

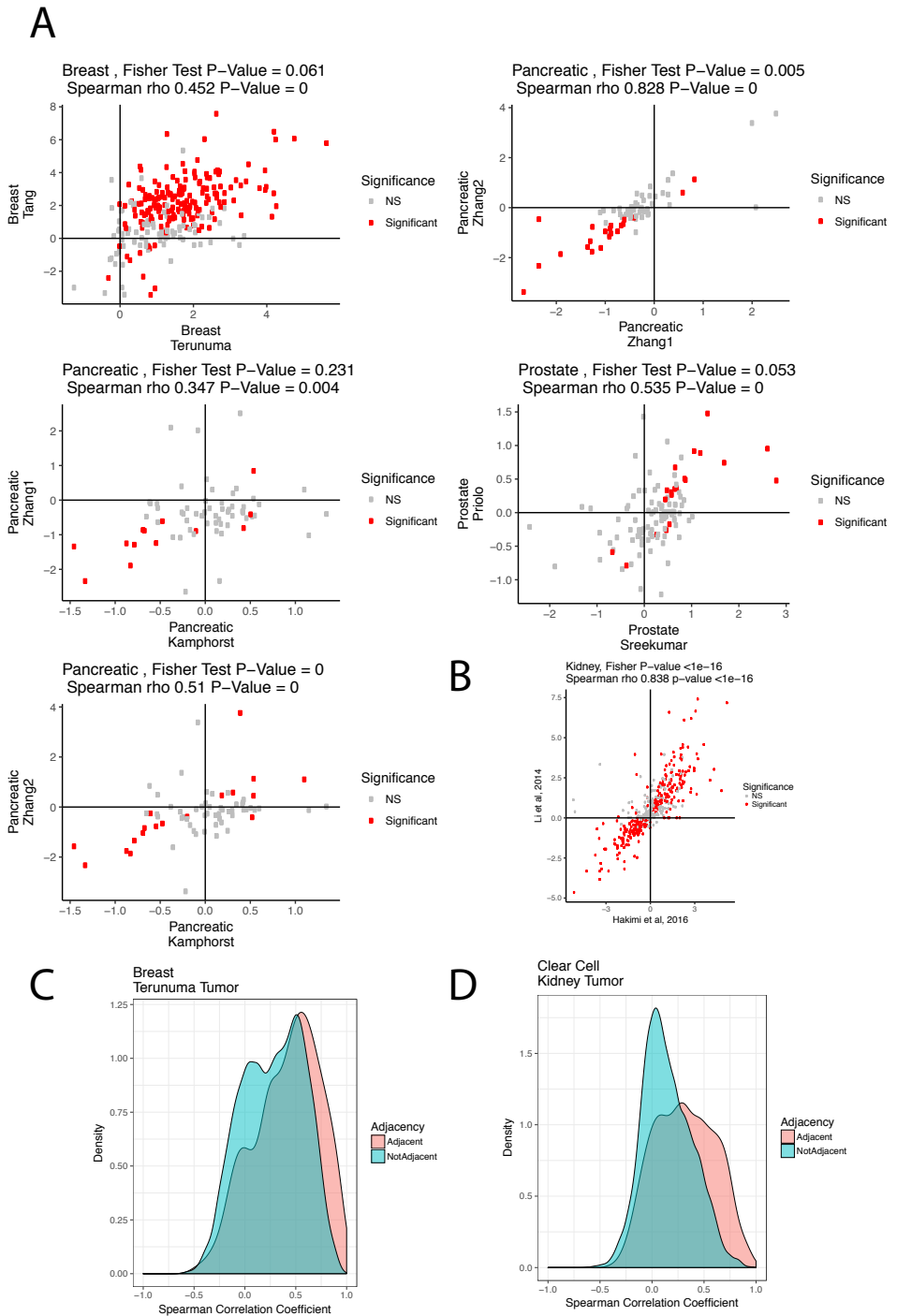


Figure S2: Comparison of differential abundance for cancer types profiled in multiple studies. **A** There exists the expectation of correlation between equivalent metabolites profiled across studies of the same cancer type. For each of the three cancer types for which we obtained profiling data from multiple studies, we compared estimates of differential abundance for common metabolites profiled in each study. Metabolites with statistically significant differential abundance are highlighted in red. Then, a Fisher's Exact Test was calculated using the number of statistically significant (red) differentially abundant metabolites within each quadrant of the shown sub-plot. The resulting p-value is presented in the title of each sub-plot. **(A)** Spearman correlation is also separately calculated for all points, regardless of statistical significance. In the cases of pancreatic cancer, there is evidence of this correlation, while in the cases of breast and prostate cancer there is a trend towards significance. **(B)** Similar to analysis above, correlation between tumor/normal differential abundance results in the Clear Cell study [35] included in this analysis, and a prior analysis [69] for which only differential abundance results were provided. **(C-D)** Comparison of distribution of Spearman correlation coefficients between metabolites which are adjacent in the metabolic network (red) and those which are not (blue) in the **(C)** Breast Terunuma ($p\text{-value } 10^{-32}$) and **(D)** Clear Cell Kidney ($p\text{-value } 10^{-59}$) studies. The observation that adjacent metabolites are more correlated to each other than non-adjacent pairs of metabolites suggests that technical noise in the metabolomics data is not excessive. Analysis was done without regard to whether tumor/normal samples were paired.

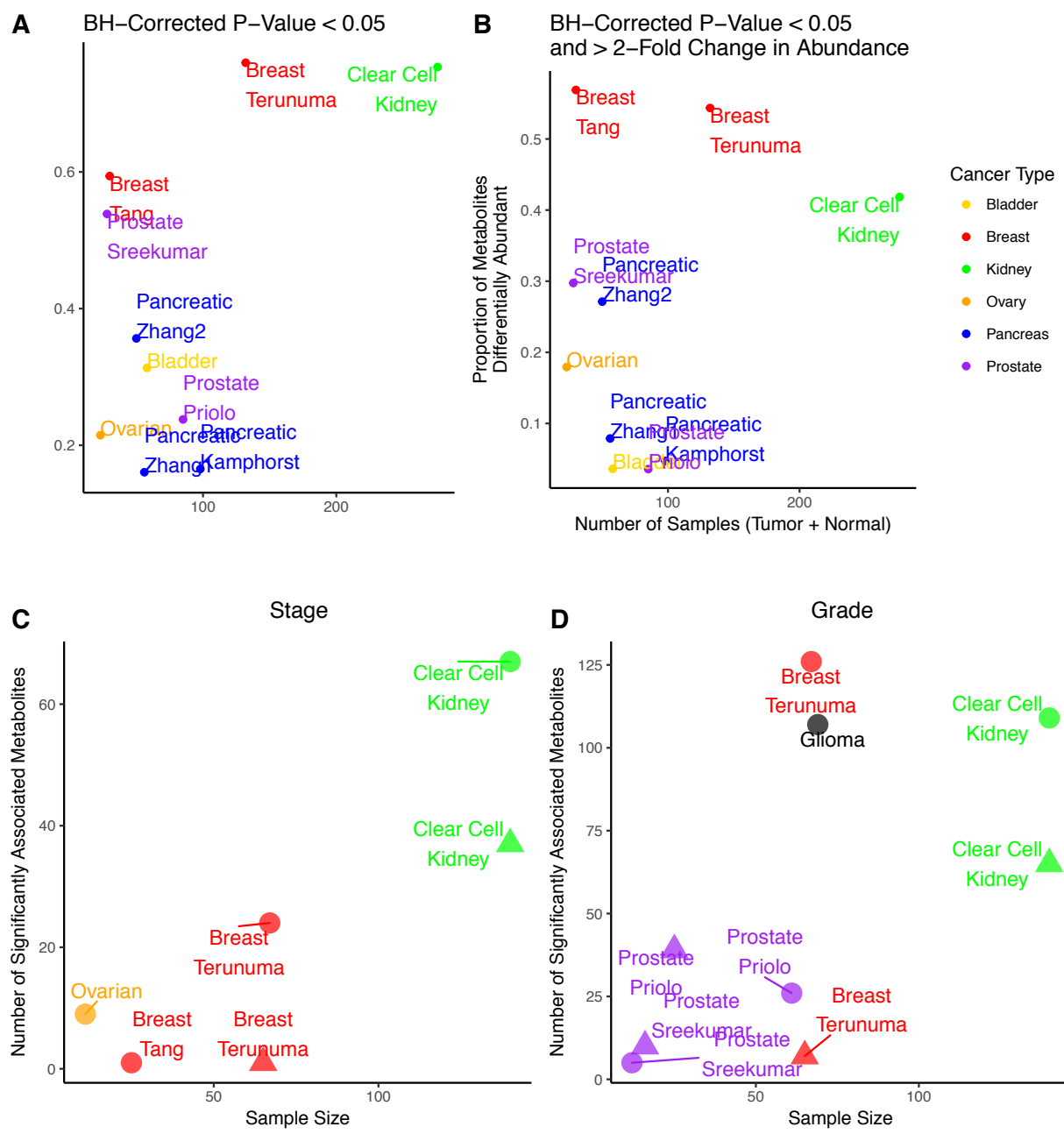


Figure S3: Proportion of differential metabolite abundance versus study sample size. (A) The proportion of metabolites measured in each study that show a statistically significant difference in abundance between tumor and normal samples versus the number of samples within each study. (B) Similar to (A), but with the additional pre-filtering for only metabolites with at least a 2-fold change in metabolite abundance. Colors denote the source tissue of individual studies. These plots provide evidence that some cancer types (e.g. pancreatic) have less differentially abundant metabolites than others (e.g. breast, kidney). In total, 10/11 studies contained adjacent-normal tissue for comparison, and were included in this analysis (in total, 482 tumor samples and 378 normal samples). (C-D) Correlation between number of metabolites found significant in clinical meta-analysis and number of samples in respective dataset. A significant correlation was found between sample size and number of statistically significant metabolites for both stage (Spearman p-value 0.06) and grade (Spearman p-value 0.02), suggesting that (at least for some cancer types) the analysis still remains underpowered. Analysis was done without regard to whether tumor/normal samples were paired.

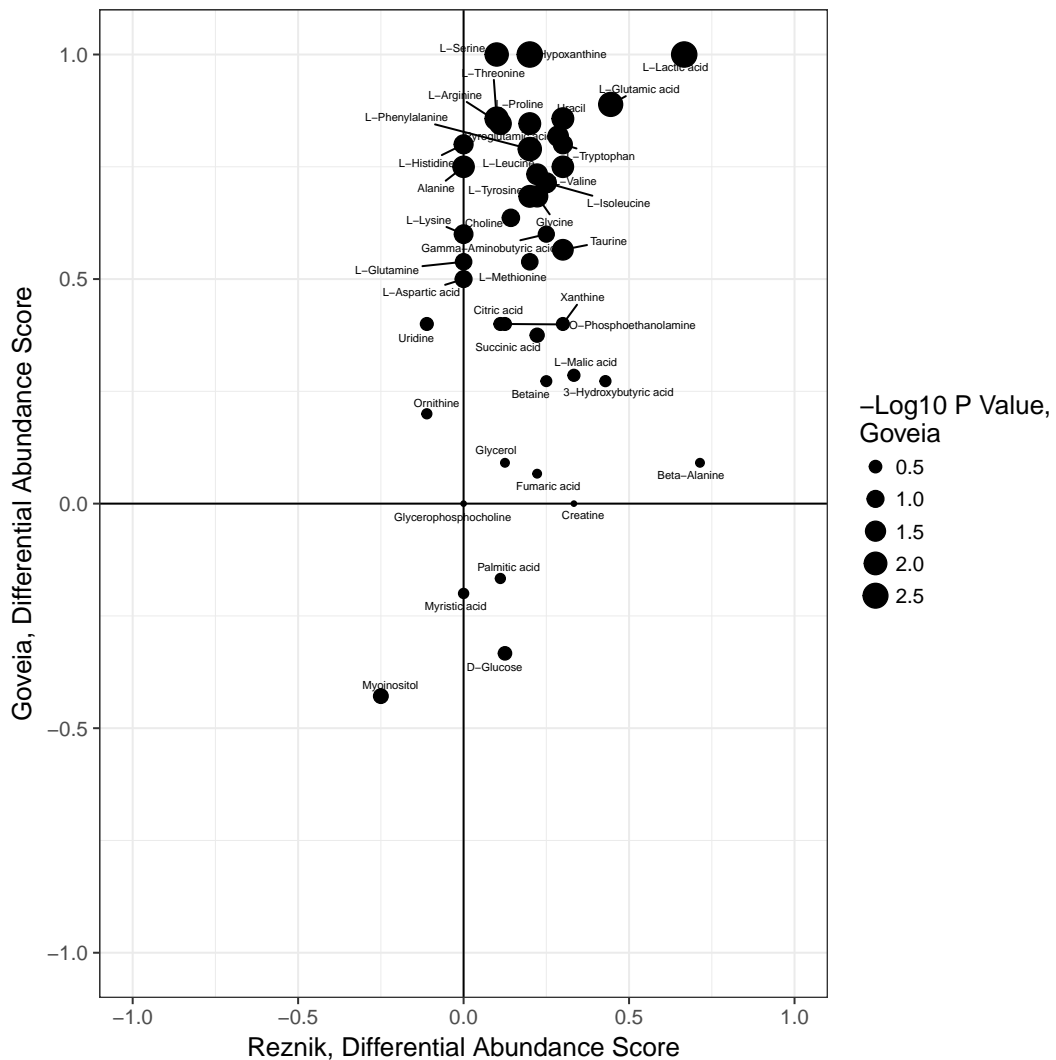


Figure S4: Comparison of differential abundance results to those from Goveia *et al.*, 2016 meta-analysis. For both our data and the data from [14], the differential abundance score is calculated as described in the Methods for Pathway Differential Abundance Score. In this case, I = number of studies with increased levels of metabolite, D = number of studies with decreased level of metabolite, S = number of studies where metabolite was measured. Pearson correlation 0.26, p-value 0.087. In total, 10/11 studies contained adjacent-normal tissue for comparison, and were included in this analysis (in total, 482 tumor samples and 378 normal samples). Analysis was done without regard to whether tumor/normal samples were paired.



Figure S5: Altered metabolic pathways across cancer studies. For each pathway and cancer study, a pathway differential abundance score is calculated (see Methods). Values less than zero are shown in blue while values greater than 0 are shown in red. The number of metabolites profiled in a given pathway and cancer study combination is denoted by the size of the circle. Pathways are sorted by their tendency to be increased/decreased in abundance in tumors compared to normal tissue. In total, 10/11 studies contained adjacent-normal tissue for comparison, and were included in this analysis (in total, 482 tumor samples and 378 normal samples). Analysis was done without regard to whether tumor/normal samples were paired.

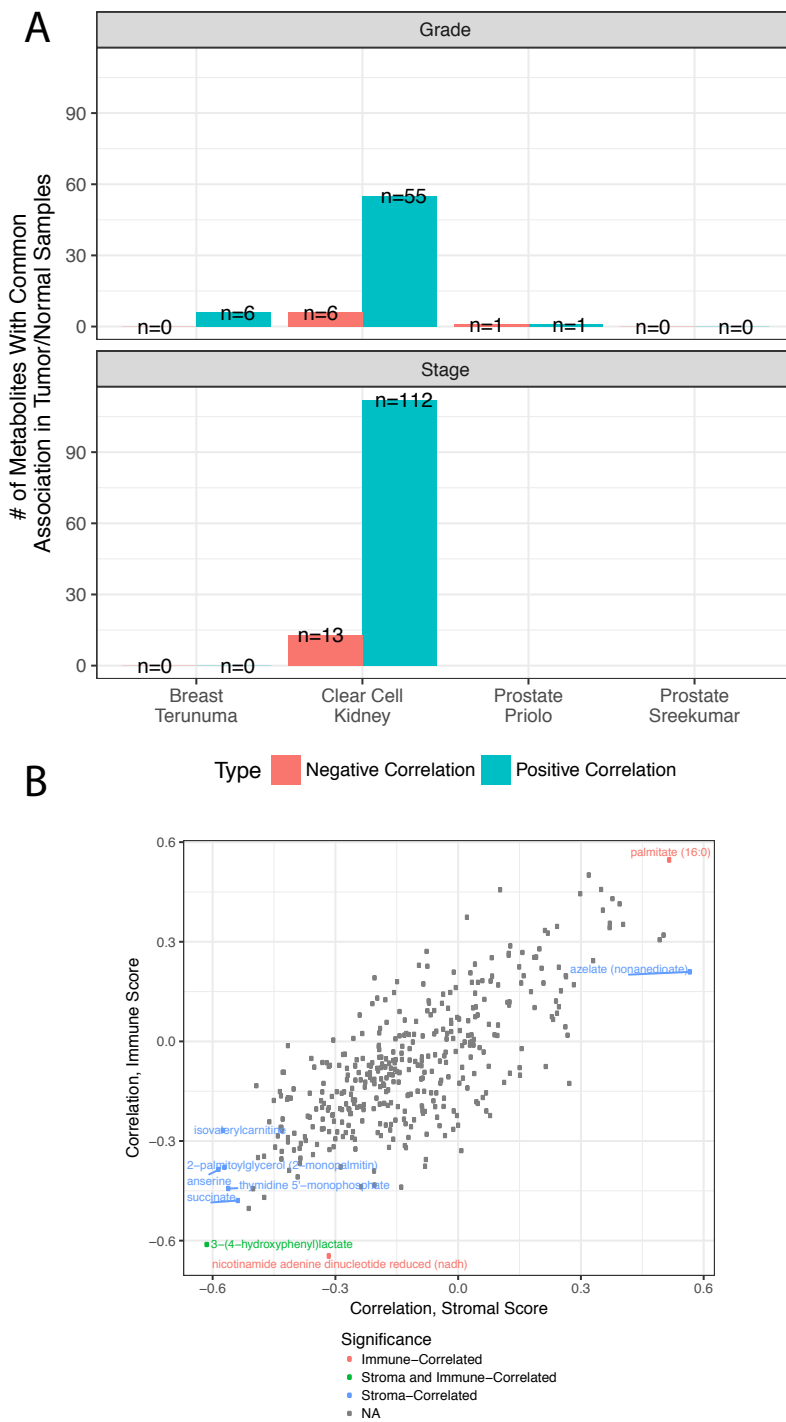


Figure S6: **A** Counts of metabolites which show a common association with clinical features (tumor grade or stage) in both tumor and normal samples. A total of 638 of the tissue samples had some type of associated clinical data (392 tumors and 246 normal tissues from 7 studies, including Breast Terunuma, Breast Tang, Kidney, Glioma, Ovarian, Prostate Priolo, and Prostate Sreekumar). Analysis was done without regard to whether tumor/normal samples were paired. **B** Correlation between metabolite levels and estimates of stromal and immune infiltration. Analysis performed over 23 TCGA samples profiled in the Breast Tang study, using estimates of stromal/immune infiltration from [70]. No metabolites were significant upon multiple-hypothesis correction (BH-adjusted $p < 0.05$), but several had unadjusted p -values < 0.01 (highlighted in the figure) and could serve as candidates for future investigation.

562 **References**

- 563 1. Giovanni Ciriello, Martin L Miller, Bülent Arman Aksoy, Yasin Senbabaoglu, Nikolaus
564 Schultz, and Chris Sander. Emerging landscape of oncogenic signatures across human can-
565 cers. *Nature genetics*, 45(10):1127–33, oct 2013.
- 566 2. Douglas Hanahan and Robert A Weinberg. Hallmarks of cancer: the next generation. *Cell*,
567 144(5):646–74, mar 2011.
- 568 3. Matthew G Vander Heiden, Lewis C Cantley, and Craig B Thompson. Understanding the
569 Warburg effect: the metabolic requirements of cell proliferation. *Science (New York, N.Y.)*,
570 324(5930):1029–33, may 2009.
- 571 4. Francesco Gatto, Intawat Nookaew, and Jens Nielsen. Chromosome 3p loss of heterozygosity
572 is associated with a unique metabolic network in clear cell renal carcinoma. *Proceedings of
573 the National Academy of Sciences of the United States of America*, pages 1319196111–, feb
574 2014.
- 575 5. Roland Nilsson, Mohit Jain, Nikhil Madhusudhan, Nina Gustafsson Sheppard, Laura
576 Strittmatter, Caroline Kampf, Jenny Huang, Anna Asplund, and Vamsi K Mootha. Metabolic
577 enzyme expression highlights a key role for MTHFD2 and the mitochondrial folate pathway
578 in cancer. *Nature communications*, 5:3128, jan 2014.
- 579 6. Jie Hu, Jason W Locasale, Jason H Bielas, Jacintha O’ Sullivan, Kieran Sheahan, Lewis C
580 Cantley, Matthew G Vander Heiden, and Dennis Vitkup. Heterogeneity of tumor-induced gene
581 expression changes in the human metabolic network. *Nature biotechnology*, 31(6):522–9, jun
582 2013.
- 583 7. Lucas B Sullivan, Dan Y Gui, and Matthew G Vander Heiden. Altered metabolite levels in
584 cancer: implications for tumour biology and cancer therapy. *Nature reviews. Cancer*, sep
585 2016.

- 586 8. Richard Possemato, Kevin M. Marks, Yoav D. Shaul, Michael E. Pacold, Dohoon Kim,
587 K?van? Birsoy, Shalini Sethumadhavan, Hin-Koon Woo, Hyun G. Jang, Abhishek K. Jha,
588 Walter W. Chen, Francesca G. Barrett, Nicolas Stransky, Zhi-Yang Tsun, Glenn S. Cowley,
589 Jordi Barretina, Nada Y. Kalaany, Peggy P. Hsu, Kathleen Ottina, Albert M. Chan, Bingbing
590 Yuan, Levi A. Garraway, David E. Root, Mari Mino-Kenudson, Elena F. Brachtel, Edward M.
591 Driggers, and David M. Sabatini. Functional genomics reveal that the serine synthesis path-
592 way is essential in breast cancer. *Nature*, 476(7360):346–350, aug 2011.
- 593 9. Andrew R Mullen, William W Wheaton, Eunsook S Jin, Pei-Hsuan Chen, Lucas B Sullivan,
594 Tzuling Cheng, Youfeng Yang, W Marston Linehan, Navdeep S Chandel, and Ralph J DeBer-
595 ardinis. Reductive carboxylation supports growth in tumour cells with defective mitochondria.
596 *Nature*, 481(7381):385–8, jan 2012.
- 597 10. Christopher T Hensley, Brandon Faubert, Qing Yuan, Naama Lev-Cohain, Eunsook Jin,
598 Jiyeon Kim, Lei Jiang, Bookyung Ko, Rachael Skelton, Laurin Loudat, Michelle Wodzak,
599 Claire Klimko, Elizabeth McMillan, Yasmeen Butt, Min Ni, Dwight Oliver, Jose Torre-
600 alba, Craig R Malloy, Kemp Kernstine, Robert E Lenkinski, Ralph J DeBerardinis, L.K.
601 Boroughs, R.J. DeBerardinis, J.M. Buescher, M.R. Antoniewicz, L.G. Boros, S.C. Burgess,
602 H. Brunengraber, C.B. Clish, R.J. DeBerardinis, O. Feron, C. Frezza, B. Ghesquiere, Et Al.,
603 P. Caro, A.U. Kishan, E. Norberg, I.A. Stanley, B. Chapuy, S.B. Ficarro, K. Polak, D. Ton-
604 dera, J. Gounarides, H. Yin, Et Al., T. Cheng, J. Suderth, C. Yang, A.R. Mullen, E.S. Jin,
605 J.M. Matés, R.J. DeBerardinis, S.M. Davidson, T. Papagiannakopoulos, B.A. Olenchock,
606 J.E. Heyman, M.A. Keibler, A. Luengo, M.R. Bauer, A.K. Jha, J.P. O'Brien, K.A. Pierce,
607 Et Al., R.J. DeBerardinis, J.J. Lum, G. Hatzivassiliou, C.B. Thompson, M. Eilertsen, S. An-
608 dersen, S. Al-Saad, Y. Kiselev, T. Donnem, H. Stenvold, I. Pettersen, K. Al-Shibli, E. Richard-
609 sen, L.T. Busund, R.M. Bremnes, T.W. Fan, A.N. Lane, R.M. Higashi, M.A. Farag, H. Gao,
610 M. Bousamra, D.M. Miller, J.W. Fletcher, B. Djulbegovic, H.P. Soares, B.A. Siegel, V.J.
611 Lowe, G.H. Lyman, R.E. Coleman, R. Wahl, J.C. Paschold, N. Avril, Et Al., P. Gao, I. Tch-

ernyshyov, T.-C. Chang, Y.-S. Lee, K. Kita, T. Ochi, K.I. Zeller, A.M. De Marzo, J.E. Van Eyk, J.T. Mendell, C.V. Dang, R.A. Gatenby, R.J. Gillies, F. Guillaumond, J. Leca, O. Olivares, M.-N. Lavaut, N. Vidal, P. Berthezène, N.J. Dusetti, C. Loncle, E. Calvo, O. Turrini, Et Al., D. Hanahan, R.A. Weinberg, H. Ji, M.R. Ramsey, D.N. Hayes, C. Fan, K. McNamara, P. Kozlowski, C. Torrice, M.C. Wu, T. Shimamura, S.A. Perera, Et Al., K.M. Kennedy, P.M. Scarbrough, A. Ribeiro, R. Richardson, H. Yuan, P. Sonveaux, C.D. Landon, J.T. Chi, S. Pizzo, T. Schroeder, M.W. Dewhirst, D.M. Koh, D.J. Collins, E.A. Maher, I. Marin-Valencia, R.M. Bachoo, T. Mashimo, J. Raisanen, K.J. Hatanpaa, A. Jindal, F.M. Jeffrey, C. Choi, C. Madden, Et Al., I. Marin-Valencia, C. Yang, T. Mashimo, S. Cho, H. Baek, X.-L. Yang, K.N. Rajagopalan, M. Maddie, V. Vemireddy, Z. Zhao, Et Al., T. Mashimo, K. Pichumani, V. Vemireddy, K.J. Hatanpaa, D.K. Singh, S. Sirasanagandla, S. Nannepaga, S.G. Piccirillo, Z. Kovacs, C. Foong, Et Al., M.L. McCleland, A.S. Adler, L. Deming, E. Cosino, L. Lee, E.M. Blackwood, M. Solon, J. Tao, L. Li, D. Shames, Et Al., C.S. Ng, D.L. Raunig, E.F. Jackson, E.A. Ashton, F. Kelcz, K.B. Kim, R. Kurzrock, T.M. McShane, T.D. Nguyen-Kim, T. Frauenfelder, K. Strobel, P. Veit-Haibach, M.W. Huellner, S. Pavlides, D. Whitaker-Menezes, R. Castello-Cros, N. Flomenberg, A.K. Witkiewicz, P.G. Frank, M.C. Casimiro, C. Wang, P. Fortina, S. Addya, Et Al., R. Possemato, K.M. Marks, Y.D. Shaul, M.E. Paold, D. Kim, K. Birsoy, S. Sethumadhavan, H.K. Woo, H.G. Jang, A.K. Jha, Et Al., K.N. Rajagopalan, R.A. Egnatchik, M.A. Calvaruso, A.T. Wasti, M.S. Padanad, L.K. Boroughs, B. Ko, C.T. Hensley, M. Acar, Z. Hu, Et Al., K. Sellers, M.P. Fox, M. Bousamra, S.P. Slone, R.M. Higashi, D.M. Miller, Y. Wang, J. Yan, M.O. Yunneva, R. Deshpande, Et Al., J. Son, C.A. Lyssiottis, H. Ying, X. Wang, S. Hua, M. Ligorio, R.M. Perera, C.R. Ferrone, E. Mullarky, N. Shyh-Chang, Et Al., P. Sonveaux, F. Végran, T. Schroeder, M.C. Wergin, J. Verrax, Z.N. Rabbani, C.J. De Saedeleer, K.M. Kennedy, C. Diepart, B.F. Jordan, Et Al., A. Terunuma, N. Putluri, P. Mishra, E.A. Mathé, T.H. Dorsey, M. Yi, T.A. Wallace, H.J. Issaq, M. Zhou, J.K. Killian, Et Al., M.G. Vander Heiden, O. Warburg, T.E. Yankeelov, J.C. Gore, M.O. Yunneva, T.W. Fan, T.D. Allen, R.M. Higashi, D.V. Ferraris, T. Tsukamoto, J.M. Matés, F.J.

- 639 Alonso, C. Wang, Y. Seo, and Et Al. Metabolic Heterogeneity in Human Lung Tumors. *Cell*,
640 164(4):681–94, feb 2016.
- 641 11. Chao Lu, Patrick S Ward, Gurpreet S Kapoor, Dan Rohle, Sevin Turcan, Omar Abdel-Wahab,
642 Christopher R Edwards, Raya Khanin, Maria E Figueroa, Ari Melnick, Kathryn E Wellen,
643 Donald M O’Rourke, Shelley L Berger, Timothy A Chan, Ross L Levine, Ingo K Mellinghoff,
644 and Craig B Thompson. IDH mutation impairs histone demethylation and results in a block to
645 cell differentiation. *Nature*, 483(7390):474–8, mar 2012.
- 646 12. C. Lu, S. Venneti, A. Akalin, F. Fang, P. S. Ward, R. G. DeMatteo, A. M. Intlekofer, C. Chen,
647 J. Ye, M. Hameed, K. Nafa, N. P. Agaram, J. R. Cross, R. Khanin, C. E. Mason, J. H. Healey,
648 S. W. Lowe, G. K. Schwartz, A. Melnick, and C. B. Thompson. Induction of sarcomas by
649 mutant IDH2. *Genes & Development*, 27(18):1986–1998, sep 2013.
- 650 13. Jared R. Mayers, Margaret E. Torrence, Laura V. Danai, Thales Papagiannakopoulos,
651 Shawn M. Davidson, Matthew R. Bauer, Allison N. Lau, Brian W. Ji, Purushottam D. Dixit,
652 Aaron M. Hosios, Alexander Muir, Christopher R. Chin, Elizaveta Freinkman, Tyler Jacks,
653 Brian M. Wolpin, Dennis Vitkup, and Matthew G. Vander Heiden. Tissue of origin dictates
654 branched-chain amino acid metabolism in mutant Kras-driven cancers. *Science*, 353(6304),
655 2016.
- 656 14. Jermaine Goveia, Andreas Pircher, Lena-Christin Conradi, Joanna Kalucka, Vincenzo La-
657 gani, Mieke Dewerchin, Guy Eelen, Ralph J DeBerardinis, Ian D Wilson, and Peter Carmeliet.
658 Meta-analysis of clinical metabolic profiling studies in cancer: challenges and opportunities.
659 *EMBO molecular medicine*, 8(10):1134–1142, oct 2016.
- 660 15. Ralph J DeBerardinis and Navdeep S Chandel. Fundamentals of cancer metabolism. *Science*
661 *advances*, 2(5):e1600200, may 2016.

- 662 16. Natalya N. Pavlova and Craig B. Thompson. The Emerging Hallmarks of Cancer Metabolism.
663 *Cell Metabolism*, 23(1):27–47, 2016.
- 664 17. Llewellyn E Jalbert, Adam Elkhaled, Joanna J Phillips, Evan Neill, Aurelia Williams, Jason C
665 Crane, Marram P Olson, Annette M Molinaro, Mitchel S Berger, John Kurhanewicz, Sab-
666 rina M Ronen, Susan M Chang, and Sarah J Nelson. Metabolic Profiling of IDH Mutation and
667 Malignant Progression in Infiltrating Glioma. *Scientific reports*, 7:44792, mar 2017.
- 668 18. Syed Haider, Alan McIntyre, Ruud G. P. M. van Stiphout, Laura M. Winchester, Simon Wig-
669 field, Adrian L. Harris, and Francesca M. Buffa. Genomic alterations underlie a pan-cancer
670 metabolic shift associated with tumour hypoxia. *Genome Biology*, 17(1):140, dec 2016.
- 671 19. Brian C Grabiner, Valentina Nardi, KÄsvanc Birsoy, Richard Possemato, Kuang Shen, Sumi
672 Sinha, Alexander Jordan, Andrew H Beck, and David M Sabatini. A diverse array of cancer-
673 associated MTOR mutations are hyperactivating and can predict rapamycin sensitivity. *Can-
674 cer discovery*, 4(5):554–63, may 2014.
- 675 20. Kevin Cho, Nathaniel G Mahieu, Stephen L Johnson, and Gary J Patti. After the feature pre-
676 sentation: technologies bridging untargeted metabolomics and biology. *Current opinion in
677 biotechnology*, 28:143–8, aug 2014.
- 678 21. Sunghwan Kim, Paul A. Thiessen, Evan E. Bolton, Jie Chen, Gang Fu, Asta Gindulyte, Liyan
679 Han, Jane He, Siqian He, Benjamin A. Shoemaker, Jiayao Wang, Bo Yu, Jian Zhang, and
680 Stephen H. Bryant. PubChem Substance and Compound databases. *Nucleic Acids Research*,
681 44(D1):D1202–D1213, jan 2016.
- 682 22. David S Wishart, Dan Tzur, Craig Knox, Roman Eisner, An Chi Guo, Nelson Young, Dean
683 Cheng, Kevin Jewell, David Arndt, Summit Sawhney, Chris Fung, Lisa Nikolai, Mike Lewis,
684 Marie-Aude Coutouly, Ian Forsythe, Peter Tang, Savita Shrivastava, Kevin Jeroncic, Paul
685 Stothard, Godwin Amegbey, David Block, David D Hau, James Wagner, Jessica Miniaci,

- 686 Melisa Clements, Mulu Gebremedhin, Natalie Guo, Ying Zhang, Gavin E Duggan, Glen D
687 Macinnis, Alim M Weljie, Reza Dowlatabadi, Fiona Bamforth, Derrick Clive, Russ Greiner,
688 Liang Li, Tom Marrie, Brian D Sykes, Hans J Vogel, and Lori Querengesser. HMDB: the
689 Human Metabolome Database. *Nucleic acids research*, 35(Database issue):D521–6, jan 2007.
- 690 23. Minoru Kanehisa, Yoko Sato, Masayuki Kawashima, Miho Furumichi, and Mao Tanabe.
691 KEGG as a reference resource for gene and protein annotation. *Nucleic acids research*,
692 44(D1):D457–62, jan 2016.
- 693 24. Atsushi Terunuma, Nagireddy Putluri, Prachi Mishra, Ewy A Mathé, Tiffany H Dorsey, Ming
694 Yi, Tiffany A Wallace, Haleem J Issaq, Ming Zhou, J Keith Killian, Holly S Stevenson, Ed-
695 ward D Karoly, King Chan, Susmita Samanta, DaRue Prieto, Tiffany Y T Hsu, Sarah J Kur-
696 ley, Vasanta Putluri, Rajni Sonavane, Daniel C Edelman, Jacob Wulff, Adrienne M Starks,
697 Yinmeng Yang, Rick A Kittles, Harry G Yfantis, Dong H Lee, Olga B Ioffe, Rachel Schiff,
698 Robert M Stephens, Paul S Meltzer, Timothy D Veenstra, Thomas F Westbrook, Arun Sreeku-
699 mar, and Stefan Ambs. MYC-driven accumulation of 2-hydroxyglutarate is associated with
700 breast cancer prognosis. *The Journal of clinical investigation*, 124(1):398–412, jan 2014.
- 701 25. Xiaohu Tang, Chao-Chieh Lin, Ivan Spasojevic, Edwin S Iversen, Jen-Tsan Chi, and Jeffrey R
702 Marks. A joint analysis of metabolomics and genetics of breast cancer. *Breast cancer research*
703 : BCR, 16(4):415, jan 2014.
- 704 26. Michael S. Lawrence, Petar Stojanov, Craig H. Mermel, James T. Robinson, Levi A. Gar-
705 raway, Todd R. Golub, Matthew Meyerson, Stacey B. Gabriel, Eric S. Lander, and Gad
706 Getz. Discovery and saturation analysis of cancer genes across 21 tumour types. *Nature*,
707 505(7484):495–501, jan 2014.
- 708 27. Yiqun Zhang, Patrick Kwok-Shing Ng, Melanie Kucherlapati, Fengju Chen, Yuexin Liu,
709 Yiu Huen Tsang, Guillermo de Velasco, Kang Jin Jeong, Rehan Akbani, Angela Hadjipanayis,
710 Angeliki Pantazi, Christopher A. Bristow, Eunjung Lee, Harshad S. Mahadeshwar, Jiabin

- 711 Tang, Jianhua Zhang, Lixing Yang, Sahil Seth, Semin Lee, Xiaojia Ren, Xingzhi Song, Huan-
712 dong Sun, Jonathan Seidman, Lovelace J. Luquette, Ruibin Xi, Lynda Chin, Alexei Pro-
713 topov, Thomas F. Westbrook, Carl Simon Shelley, Toni K. Choueiri, Michael Ittmann,
714 Carter Van Waes, John N. Weinstein, Han Liang, Elizabeth P. Henske, Andrew K. Godwin,
715 Peter J. Park, Raju Kucherlapati, Kenneth L. Scott, Gordon B. Mills, David J. Kwiatkowski,
716 and Chad J. Creighton. A Pan-Cancer Proteogenomic Atlas of PI3K/AKT/mTOR Pathway
717 Alterations. *Cancer Cell*, 31(6):820–832.e3, jun 2017.
- 718 28. Barbara A. Conley and James H. Doroshow. Molecular Analysis for Therapy Choice: NCI
719 MATCH. *Seminars in Oncology*, 41(3):297–299, jun 2014.
- 720 29. Michael Platten, Wolfgang Wick, and Benoît J Van den Eynde. Tryptophan catabolism in
721 cancer: beyond IDO and tryptophan depletion. *Cancer research*, 72(21):5435–40, nov 2012.
- 722 30. Maria Laura Belladonna, Paolo Puccetti, Ciriana Orabona, Francesca Fallarino, Carmine
723 Vacca, Claudia Volpi, Stefania Gizzi, Maria Teresa Pallotta, Maria Cristina Fioretti, and Ur-
724 sula Grohmann. Immunosuppression via tryptophan catabolism: the role of kynurenine path-
725 way enzymes. *Transplantation*, 84(1 Suppl):S17–20, jul 2007.
- 726 31. Yiquan Chen and Gilles J Guillemin. Kynurenine pathway metabolites in humans: disease and
727 healthy States. *International journal of tryptophan research : IJTR*, 2:1–19, 2009.
- 728 32. Augustin Luna, Özgün Babur, Bülent Arman Aksoy, Emek Demir, and Chris Sander. Pax-
729 toolsR: pathway analysis in R using Pathway Commons. *Bioinformatics*, 32(8):1262–1264,
730 apr 2016.
- 731 33. Ethan G Cerami, Benjamin E Gross, Emek Demir, Igor Rodchenkov, Ozgün Babur, Nadia An-
732 war, Nikolaus Schultz, Gary D Bader, and Chris Sander. Pathway Commons, a web resource
733 for biological pathway data. *Nucleic acids research*, 39(Database issue):D685–90, jan 2011.

- 734 34. Vivian Law, Craig Knox, Yannick Djoumbou, Tim Jewison, An Chi Guo, Yifeng Liu, Adam
735 Maciejewski, David Arndt, Michael Wilson, Vanessa Neveu, Alexandra Tang, Geraldine
736 Gabriel, Carol Ly, Sakina Adamjee, Zerihun T Dame, Beomsoo Han, You Zhou, and David S
737 Wishart. DrugBank 4.0: shedding new light on drug metabolism. *Nucleic acids research*,
738 42(Database issue):D1091–7, jan 2014.
- 739 35. A.A. Hakimi, E. Reznik, C.-H. Lee, C.J. Creighton, A.R. Brannon, A. Luna, B.A. Aksoy,
740 E.M. Liu, R. Shen, W. Lee, Y. Chen, S.M. Stirdvant, P. Russo, Y.-B. Chen, S.K. Tickoo, V.E.
741 Reuter, E.H. Cheng, C. Sander, and J.J. Hsieh. An Integrated Metabolic Atlas of Clear Cell
742 Renal Cell Carcinoma. *Cancer Cell*, 29(1):104–116, 2016.
- 743 36. Simendra Singh, Amir R Khan, and Alok K Gupta. Role of glutathione in cancer patho-
744 physiology and therapeutic interventions. *Journal of experimental therapeutics & oncology*,
745 9(4):303–16, 2012.
- 746 37. Ed Reznik, Pankaj Mehta, and Daniel Segrè. Flux Imbalance Analysis and the Sensitiv-
747 ity of Cellular Growth to Changes in Metabolite Pools. *PLoS Computational Biology*,
748 9(8):e1003195, aug 2013.
- 749 38. Luca Gerosa, Bart R.B. Haverkorn van Rijsewijk, Dimitris Christodoulou, Karl Kochanowski,
750 Thomas S.B. Schmidt, Elad Noor, and Uwe Sauer. Pseudo-transition Analysis Identifies the
751 Key Regulators of Dynamic Metabolic Adaptations from Steady-State Data. *Cell Systems*,
752 1(4):270–282, 2015.
- 753 39. Marshall Louis Reaves, Brian D Young, Aaron M Hosios, Yi-Fan Xu, and Joshua D Rabi-
754 nowitz. Pyrimidine homeostasis is accomplished by directed overflow metabolism. *Nature*,
755 500(7461):237–41, aug 2013.

- 756 40. Keshav K Singh, Mohamed M Desouki, Renty B Franklin, and Leslie C Costello. Mitochondrial aconitase and citrate metabolism in malignant and nonmalignant human prostate tissues.
757
758 *Molecular cancer*, 5:14, apr 2006.
- 759 41. E. Reznik, M.L. Miller, Y. ÅdenbabaoÄ§lu, N. Riaz, J. Sarungbam, S.K. Tickoo, H.A. Al-
760 Ahmadie, W. Lee, V.E. Seshan, A.A. Hakimi, and C. Sander. Mitochondrial DNA copy num-
761 ber variation across human cancers. *eLife*, 5(FEBRUARY2016), 2016.
- 762 42. Ed Reznik, Qingguo Wang, Konnor La, Nikolaus Schultz, and Chris Sander. Mitochondrial
763 respiratory gene expression is suppressed in many cancers. *eLife*, 6, jan 2017.
- 764 43. Marion I Menzel, Eliane V Farrell, Martin A Janich, Oleksandr Khegai, Florian Wiesinger,
765 Stephan Nekolla, Angela M Otto, Axel Haase, Rolf F Schulte, and Markus Schwaiger. Mul-
766 timodal assessment of in vivo metabolism with hyperpolarized [1-13C]MR spectroscopy and
767 18F-FDG PET imaging in hepatocellular carcinoma tumor-bearing rats. *Journal of nuclear*
768 *medicine : official publication, Society of Nuclear Medicine*, 54(7):1113–9, jul 2013.
- 769 44. S. Mandal, A. Mandal, H. E. Johansson, A. V. Orjalo, and M. H. Park. Depletion of cellular
770 polyamines, spermidine and spermine, causes a total arrest in translation and growth in mam-
771 malian cells. *Proceedings of the National Academy of Sciences*, 110(6):2169–2174, feb 2013.
- 772 45. Guro F. Giskeødegård, Helena Bertilsson, Kirsten M. Selnæs, Alan J. Wright, Tone F. Ba-
773 then, Trond Viset, Jostein Halgunset, Anders Angelsen, Ingrid S. Gribbestad, and May-Britt
774 Tessem. Spermine and Citrate as Metabolic Biomarkers for Assessing Prostate Cancer Ag-
775 gressiveness. *PLoS ONE*, 8(4):e62375, apr 2013.
- 776 46. Andrew M Intlekofer, Bo Wang, Hui Liu, Hardik Shah, Carlos Carmona-Fontaine, Ari?n S
777 Rustenburg, Salah Salah, M R Gunner, John D Chodera, Justin R Cross, and Craig B Thomp-
778 son. L-2-Hydroxyglutarate production arises from noncanonical enzyme function at acidic
779 pH. *Nature Chemical Biology*, 13(5):494–500, mar 2017.

- 780 47. E.-H. Shim, C. B. Livi, D. Rakheja, J. Tan, D. Benson, V. Parekh, E.-Y. Kho, A. P. Ghosh,
781 R. Kirkman, S. Velu, S. Dutta, B. Chenna, S. L. Rea, R. J. Mishur, Q. Li, T. L. Johnson-Pais,
782 L. Guo, S. Bae, S. Wei, K. Block, and S. Sudarshan. L-2-Hydroxyglutarate: An Epigenetic
783 Modifier and Putative Oncometabolite in Renal Cancer. *Cancer Discovery*, 4(11):1290–1298,
784 nov 2014.
- 785 48. Nam Trung Nguyen, Taisuke Nakahama, Duc Hoang Le, Le Van Son, Ha Hoang Chu, and
786 Tadamitsu Kishimoto. Aryl hydrocarbon receptor and kynurenone: recent advances in autoim-
787 mune disease research. *Frontiers in immunology*, 5:551, oct 2014.
- 788 49. S.-C. Chuang, A. Fanidi, P. M. Ueland, C. Relton, O. Midttun, S. E. Vollset, M. J. Gunter,
789 M. J. Seckl, R. C. Travis, N. Wareham, A. Trichopoulou, P. Lagiou, D. Trichopoulos, P. H. M.
790 Peeters, H. B. Bueno-de Mesquita, H. Boeing, A. Wientzek, T. Kuehn, R. Kaaks, R. Tu-
791 mino, C. Agnoli, D. Palli, A. Naccarati, E. A. Aicua, M.-J. Sanchez, J. R. Quiros, M.-
792 D. Chirlaque, A. Agudo, M. Johansson, K. Grankvist, M.-C. Boutron-Ruault, F. Clavel-
793 Chapelon, G. Fagherazzi, E. Weiderpass, E. Riboli, P. J. Brennan, P. Vineis, and M. Johans-
794 son. Circulating Biomarkers of Tryptophan and the Kynurenone Pathway and Lung Cancer
795 Risk. *Cancer Epidemiology Biomarkers & Prevention*, 23(3):461–468, mar 2014.
- 796 50. Chai K. Lim, Ayse Bilgin, David B. Lovejoy, Vanessa Tan, Sonia Bustamante, Bruce V.
797 Taylor, Alban Bessede, Bruce J. Brew, and Gilles J. Guillemain. Kynurenone pathway
798 metabolomics predicts and provides mechanistic insight into multiple sclerosis progression.
799 *Scientific Reports*, 7:41473, feb 2017.
- 800 51. Benjamin Heng, Chai K Lim, David B Lovejoy, Alban Bessede, Laurence Gluch, and Gilles J
801 Guillemain. Understanding the role of the kynurenone pathway in human breast cancer im-
802 munobiology. *Oncotarget*, 7(6):6506–20, feb 2016.
- 803 52. Chih-Hao Chang, Jing Qiu, David O’Sullivan, Michael D Buck, Takuro Noguchi, Jonathan D
804 Curtis, Qiongyu Chen, Mariel Gindin, Matthew M Gubin, Gerritje J W van der Windt, Elena

805 Tond, Robert D Schreiber, Edward J Pearce, Erika L Pearce, M. Ahmadzadeh, L.A. John-
806 son, B. Heemskerk, J.R. Wunderlich, M.E. Dudley, D.E. White, S.A. Rosenberg, A. Ani-
807 chini, A. Molla, C. Vegetti, I. Bersani, R. Zappasodi, F. Arienti, F. Ravagnani, A. Maurichi,
808 R. Patuzzo, M. Santinami, Et Al., L. Baitsch, P. Baumgaertner, E. Devêvre, S.K. Raghav,
809 A. Legat, L. Barba, S. Wieckowski, H. Bouzourene, B. Deplancke, P. Romero, Et Al., A.S.
810 Berghoff, B. Kiesel, G. Widhalm, O. Rajky, G. Ricken, A. Wohrer, K. Dieckmann, M. Filip-
811 its, A. Brandstetter, M. Weller, Et Al., K. Birsoy, R. Possemato, F.K. Lorbeer, E.C. Bayrak-
812 tar, P. Thiru, B. Yucel, T. Wang, W.W. Chen, C.B. Clish, D.M. Sabatini, J.R. Brahmer,
813 S.S. Tykodi, L.Q. Chow, W.J. Hwu, S.L. Topalian, P. Hwu, C.G. Drake, L.H. Camacho,
814 J. Kauh, K. Odunsi, Et Al., R. Carlsson, S. Issazadeh-Navikas, C.M. Cham, G. Driessens,
815 J.P. O'Keefe, T.F. Gajewski, C.H. Chang, J.D. Curtis, L.B. Maggi, B. Faubert, A.V. Villar-
816 ino, D. O'Sullivan, S.C. Huang, G.J. van der Windt, J. Blagih, J. Qiu, Et Al., S. Constant,
817 C. Pfeiffer, A. Woodard, T. Pasqualini, K. Bottomly, J. Crespo, H. Sun, T.H. Welling, Z. Tian,
818 W. Zou, H. Dong, S.E. Strome, D.R. Salomao, H. Tamura, F. Hirano, D.B. Flies, P.C. Roche,
819 J. Lu, G. Zhu, K. Tamada, Et Al., C.A. Doughty, B.F. Bleiman, D.J. Wagner, F.J. Dufort, J.M.
820 Mataraza, M.F. Roberts, T.C. Chiles, E. Favaro, K. Bensaad, M.G. Chong, D.A. Tenant, D.J.
821 Ferguson, C. Snell, G. Steers, H. Turley, J.L. Li, U.L. Günther, Et Al., K. Fischer, P. Hoff-
822 mann, S. Voelkl, N. Meidenbauer, J. Ammer, M. Edinger, E. Gottfried, S. Schwarz, G. Rothe,
823 S. Hoves, Et Al., L.M. Francisco, P.T. Sage, A.H. Sharpe, K.A. Frauwirth, J.L. Riley, M.H.
824 Harris, R.V. Parry, J.C. Rathmell, D.R. Plas, R.L. Elstrom, C.H. June, C.B. Thompson, R.A.
825 Gatenby, R.J. Gillies, V.A. Gerriets, R.J. Kishton, A.G. Nichols, A.N. Macintyre, M. In-
826 oue, O. Ilkayeva, P.S. Winter, X. Liu, B. Priyadarshini, M.E. Slawinska, Et Al., J.D. Gor-
827 dan, C.B. Thompson, M.C. Simon, M.M. Gubin, X. Zhang, H. Schuster, E. Caron, J.P. Ward,
828 T. Noguchi, Y. Ivanova, J. Hundal, C.D. Arthur, W.J. Krebber, Et Al., O. Hamid, C. Robert,
829 A. Daud, F.S. Hodi, W.J. Hwu, R. Kefford, J.D. Wolchok, P. Hersey, R.W. Joseph, J.S. We-
830 ber, Et Al., M.E. Hatten, M.L. Shelanski, F.S. Hodi, S.J. O'Day, D.F. McDermott, R.W. We-
831 ber, J.A. Sosman, J.B. Haanen, R. Gonzalez, C. Robert, D. Schadendorf, J.C. Hassel, Et Al.,

832 S.C. Huang, B. Everts, Y. Ivanova, D. O'Sullivan, M. Nascimento, A.M. Smith, W. Beatty,
833 L. Love-Gregory, W.Y. Lam, C.M. O'Neill, Et Al., S. Issazadeh-Navikas, S.R. Jacobs, C.E.
834 Herman, N.J. Maciver, J.A. Wofford, H.L. Wieman, J.J. Hammen, J.C. Rathmell, M.E. Keir,
835 M.J. Butte, G.J. Freeman, A.H. Sharpe, D.H. Kim, D.D. Sarbassov, S.M. Ali, J.E. King,
836 R.R. Latek, H. Erdjument-Bromage, P. Tempst, D.M. Sabatini, K. Kingwell, A.D. Kohn,
837 A. Barthel, K.S. Kovacina, A. Boge, B. Wallach, S.A. Summers, M.J. Birnbaum, P.H. Scott,
838 J.C. Lawrence, R.A. Roth, A. Lanzavecchia, F. Sallusto, M. Laplante, D.M. Sabatini, Y. Liu,
839 R. Carlsson, M. Ambjørn, M. Hasan, W. Badn, A. Darabi, P. Siesjö, S. Issazadeh-Navikas,
840 H. Matsushita, M.D. Vesely, D.C. Koboldt, C.G. Rickert, R. Uppaluri, V.J. Magrini, C.D.
841 Arthur, J.M. White, Y.S. Chen, L.K. Shea, Et Al., A.L. Mellor, D.H. Munn, R.D. Michalek,
842 V.A. Gerriets, S.R. Jacobs, A.N. Macintyre, N.J. MacIver, E.F. Mason, S.A. Sullivan, A.G.
843 Nichols, J.C. Rathmell, M.B. Mockler, M.J. Conroy, J. Lysaght, D.H. Munn, A.L. Mellor,
844 D.H. Munn, E. Shafizadeh, J.T. Attwood, I. Bondarev, A. Pashine, A.L. Mellor, D.G. Nicholls,
845 V.M. Darley-Usmar, M. Wu, P.B. Jensen, G.W. Rogers, D.A. Ferrick, D. O'Sullivan, E.L.
846 Pearce, D.B. Page, M.A. Postow, M.K. Callahan, J.P. Allison, J.D. Wolchok, I.A. Parish,
847 S.M. Kaech, R.V. Parry, J.M. Chemnitz, K.A. Frauwirth, A.R. Lanfranco, I. Braunstein, S.V.
848 Kobayashi, P.S. Linsley, C.B. Thompson, J.L. Riley, N. Patsoukis, K. Bardhan, P. Chatter-
849 jee, D. Sari, B. Liu, L.N. Bell, E.D. Karoly, G.J. Freeman, V. Petkova, P. Seth, Et Al., E.L.
850 Pearce, M.C. Poffenberger, C.H. Chang, R.G. Jones, V.A. Pedicord, J.R. Cross, W. Montalvo-
851 Ortiz, M.L. Miller, J.P. Allison, S.A. Quezada, K.S. Peggs, R.R. Rao, Q. Li, P.A. Shrikant,
852 T.R. Simpson, F. Li, W. Montalvo-Ortiz, M.A. Sepulveda, K. Bergerhoff, F. Arce, C. Rod-
853 die, J.Y. Henry, H. Yagita, J.D. Wolchok, Et Al., S. Spranger, H.K. Koblish, B. Horton, P.A.
854 Scherle, R. Newton, T.F. Gajewski, M.K. Srivastava, P. Sinha, V.K. Clements, P. Rodriguez,
855 S. Ostrand-Rosenberg, M.M. Staron, S.M. Gray, H.D. Marshall, I.A. Parish, J.H. Chen, C.J.
856 Perry, G. Cui, M.O. Li, S.M. Kaech, D. Vats, L. Mukundan, J.I. Odegaard, L. Zhang, K.L.
857 Smith, C.R. Morel, R.A. Wagner, D.R. Greaves, P.J. Murray, A. Chawla, M.D. Vesely, R.D.
858 Schreiber, R. Wang, C.P. Dillon, L.Z. Shi, S. Milasta, R. Carter, D. Finkelstein, L.L. Mc-

- 859 Cormick, P. Fitzgerald, H. Chi, J. Munger, D.R. Green, O. Warburg, E.E. West, H.T. Jin,
860 A.U. Rasheed, P. Penalosa-Macmaster, S.J. Ha, W.G. Tan, B. Youngblood, G.J. Freeman,
861 K.A. Smith, R. Ahmed, E.J. Wherry, J.D. Wolchok, H. Kluger, M.K. Callahan, M.A. Pos-
862 tow, N.A. Rizvi, A.M. Lesokhin, N.H. Segal, C.E. Ariyan, R.A. Gordon, K. Reed, and Et Al.
863 Metabolic Competition in the Tumor Microenvironment Is a Driver of Cancer Progression.
864 *Cell*, 162(6):1229–41, sep 2015.
- 865 53. Andrew E Place, Sung Jin Huh, and Kornelia Polyak. The microenvironment in breast can-
866 cer progression: biology and implications for treatment. *Breast cancer research : BCR*,
867 13(6):227, dec 2011.
- 868 54. Daniela F Quail and Johanna A Joyce. Microenvironmental regulation of tumor progression
869 and metastasis. *Nature medicine*, 19(11):1423–37, nov 2013.
- 870 55. Robert A. Casero and Laurence J. Marton. Targeting polyamine metabolism and function in
871 cancer and other hyperproliferative diseases. *Nature Reviews Drug Discovery*, 6(5):373–390,
872 may 2007.
- 873 56. Eugene W. Gerner and Frank L. Meyskens. Polyamines and cancer: old molecules, new un-
874 derstanding. *Nature Reviews Cancer*, 4(10):781–792, oct 2004.
- 875 57. Cristovão M Sousa, Douglas E Biancur, Xiaoxu Wang, Christopher J Halbrook, Mara H Sher-
876 man, Li Zhang, Daniel Kremer, Rosa F Hwang, Agnes K Witkiewicz, Haoqiang Ying, John M
877 Asara, Ronald M Evans, Lewis C Cantley, Costas A Lyssiotis, and Alec C Kimmelman. Pan-
878 creatic stellate cells support tumour metabolism through autophagic alanine secretion. *Nature*,
879 536(7617):479–83, aug 2016.
- 880 58. E. Reznik and C. Sander. Extensive Decoupling of Metabolic Genes in Cancer. *PLoS Compu-*
881 *tational Biology*, 11(5), 2015.

- 882 59. Jurre J Kamphorst, Michel Nofal, Cosimo Commissio, Sean R Hackett, Wenyun Lu, Elda
883 Grabocka, Matthew G Vander Heiden, George Miller, Jeffrey A Drebin, Dafna Bar-Sagi,
884 Craig B Thompson, and Joshua D Rabinowitz. Human pancreatic cancer tumors are nutrient
885 poor and tumor cells actively scavenge extracellular protein. *Cancer research*, 75(3):544–53,
886 feb 2015.
- 887 60. Wei Xu, Hui Yang, Ying Liu, Ying Yang, Ping Wang, Se-Hee Kim, Shinsuke Ito, Chen Yang,
888 Pu Wang, Meng-Tao Xiao, Li-xia Liu, Wen-qing Jiang, Jing Liu, Jin-ye Zhang, Bin Wang,
889 Stephen Frye, Yi Zhang, Yan-hui Xu, Qun-ying Lei, Kun-Liang Guan, Shi-min Zhao, and Yue
890 Xiong. Oncometabolite 2-hydroxyglutarate is a competitive inhibitor of α -ketoglutarate-
891 dependent dioxygenases. *Cancer cell*, 19(1):17–30, jan 2011.
- 892 61. Prakash Chinnaiyan, Elizabeth Kensicki, Gregory Bloom, Antony Prabhu, Bhaswati Sar-
893 car, Soumen Kahali, Steven Eschrich, Xiaotao Qu, Peter Forsyth, and Robert Gillies. The
894 metabolomic signature of malignant glioma reflects accelerated anabolic metabolism. *Cancer
895 research*, 72(22):5878–88, nov 2012.
- 896 62. Miranda Y Fong, Jonathan McDunn, and Sham S Kakar. Identification of metabolites in the
897 normal ovary and their transformation in primary and metastatic ovarian cancer. *PloS one*,
898 6(5):e19963, jan 2011.
- 899 63. Geng Zhang, Peijun He, Hanson Tan, Anuradha Budhu, Jochen Gaedcke, B Michael Ghadimi,
900 Thomas Ried, Harris G Yfantis, Dong H Lee, Anirban Maitra, Nader Hanna, H Richard
901 Alexander, and S Perwez Hussain. Integration of metabolomics and transcriptomics revealed
902 a fatty acid network exerting growth inhibitory effects in human pancreatic cancer. *Clini-
903 cal cancer research : an official journal of the American Association for Cancer Research*,
904 19(18):4983–93, sep 2013.
- 905 64. Carmen Priolo, Saumyadipta Pyne, Joshua Rose, Erzsébet Ravasz Regan, Giorgia Zadra, Cor-
906 nelia Photopoulos, Stefano Cacciatore, Denise Schultz, Natalia Scaglia, Jonathan McDunn,

- 907 Angelo M De Marzo, and Massimo Loda. AKT1 and MYC induce distinctive metabolic fin-
908 gerprints in human prostate cancer. *Cancer research*, 74(24):7198–204, dec 2014.
- 909 65. Nagireddy Putluri, Ali Shojaie, Vihas T Vasu, Shaiju K Vareed, Srilatha Nalluri, Vasanta
910 Putluri, Gagan Singh Thangjam, Katrin Panzitt, Christopher T Tallman, Charles Butler,
911 Theodore R Sana, Steven M Fischer, Gabriel Sica, Daniel J Brat, Huidong Shi, Ganesh S
912 Palapattu, Yair Lotan, Alon Z Weizer, Martha K Terris, Shahrokh F Shariat, George Michai-
913 lidis, and Arun Sreekumar. Metabolomic profiling reveals potential markers and bioprocesses
914 altered in bladder cancer progression. *Cancer research*, 71(24):7376–86, dec 2011.
- 915 66. Arun Sreekumar, Laila M Poisson, Thekkelnaycke M Rajendiran, Amjad P Khan, Qi Cao, Jin-
916 dan Yu, Bharathi Laxman, Rohit Mehra, Robert J Lonigro, Yong Li, Mukesh K Nyati, Aarif
917 Ahsan, Shanker Kalyana-Sundaram, Bo Han, Xuhong Cao, Jaeman Byun, Gilbert S Omenn,
918 Debashis Ghosh, Subramaniam Pennathur, Danny C Alexander, Alvin Berger, Jeffrey R Shus-
919 ter, John T Wei, Sooryanarayana Varambally, Christopher Beecher, and Arul M Chinnaiyan.
920 Metabolomic profiles delineate potential role for sarcosine in prostate cancer progression. *Nature*,
921 457(7231):910–4, feb 2009.
- 922 67. Gert Wohlgemuth, Pradeep Kumar Haldiya, Egon Willighagen, Tobias Kind, and Oliver
923 Fiehn. The Chemical Translation Service—a web-based tool to improve standardization of
924 metabolomic reports. *Bioinformatics (Oxford, England)*, 26(20):2647–8, oct 2010.
- 925 68. Thomas M. Loughin. A systematic comparison of methods for combining p-values from inde-
926 pendent tests. *Computational Statistics & Data Analysis*, 47(3):467–485, 2004.
- 927 69. Bo Li, Bo Qiu, David S. M. Lee, Zandra E. Walton, Joshua D. Ochocki, Lijoy K. Mathew,
928 Anthony Mancuso, Terence P. F. Gade, Brian Keith, Itzhak Nissim, and M. Celeste Simon.
929 Fructose-1,6-bisphosphatase opposes renal carcinoma progression. *Nature*, 513(7517):251–
930 255, jul 2014.

931 70. Kosuke Yoshihara, Maria Shahmoradgoli, Emmanuel Martínez, Rahulsimham Vege, Hoon
932 Kim, Wandaliz Torres-Garcia, Victor Treviño, Hui Shen, Peter W Laird, Douglas A Levine,
933 Scott L Carter, Gad Getz, Katherine Stemke-Hale, Gordon B Mills, and Roel G W Verhaak.
934 Inferring tumour purity and stromal and immune cell admixture from expression data. *Nature*
935 *communications*, 4:2612, jan 2013.

936 **Acknowledgements**

937 We would like to thank each of the original investigators and their teams who contributed their
938 data to this work and kindly offered us their feedback, including but not limited to James Hsieh
939 (kidney), Stefan Ambs (breast), Jeffrey R. Marks (breast), Max Loda (prostate), Arun Sreekumar
940 (bladder), Josh Rabinowitz (pancreatic), Prakash Chinnaiyan (glioma), Arul Chinnaiyan (prostate),
941 S. Pervez Hussain (pancreatic), and Sham Kakar (ovarian). The work was supported by Ruth L.
942 Kirschstein National Research Service Award (grant no. F32 CA192901 to AL), and the National
943 Resource for Network Biology (NRNB) from the National Institute of General Medical Sciences
944 (NIGMS) (grant no. P41 GM103504 to CS). CJC was supported by NIH grant CA125123.